NASA
National Aeronautics and
Space Administration

Draft

Lyndon B. Johnson Space Center
Houston, Texas 77058

STRATEGIC DEFENSE INITIATIVE (SDI)
ORBITAL DEBRIS CONSIDERATION

Job Order 66-520

Prepared By

Lockheed Engineering and Management Services Company, Inc.
Houston, Texas

Contract NAS 9-15800

For

SOLAR SYSTEM EXPLORATION DIVISION
SPACE AND LIFE SCIENCES DIRECTORATE

August 1985

LEMSCO-21807

Addendum to Draft, August 22, 2012

A formal presentation of this report was given to General Abrahamson, Director of the Strategic Defense Initiative Organization (SDIO) by Joe Loftus and Don Kessler (NASA) on September 27, 1985, and a number of copies of the final report were left for SDIO's consideration. The only surviving copy of the report within NASA is this draft and a copy of the bound final report that I have in my files. Minor changes to the draft were included in the final report, but the technical content and conclusions were unchanged.

Shortly afterwards, the SDIO dropped the constellation architecture described in the report in favor of a concept called "Brilliant Pebbles", which consisted of smaller satellites at a lower altitude. Smaller satellites reduced the probability of collisions and the lower altitude ensured that any fragments resulting from any collision would quickly decay from orbit, avoiding the issues described in this report.

However, the report remains valuable since it illustrates an extreme constellation concept which can quickly cascade out of control. The report concludes that the addition of shielding shortens the life of constellation satellites and produces and an even larger long-term hazard for all satellites attempting to operate in the region … possibly for centuries, depending on the altitude of the constellation.

NASA has constructed more sophisticated models that tend to confirm most predictions of this model. For example, Figure 7-4 predicts four collisions between objects larger than 10 cm by 2012. That is what is predicted by current models and is also what has been observed. On the other hand, the newer models offer better resolution based on more data, so there are differences. For example, although the 1 cm flux measured by the Haystack radar is very close to that predicted in Figure 7-2, the altitude distribution between 500 and 1000 km is different. Therefore, it is highly recommended that any planners of a future large constellation coordinate with the Orbital Debris Program Office at NASA to provide a realistic long-term assessment of their plan.

Don Kessler

STRATEGIC DEFENSE INITIATIVE (SDI)
ORBITAL DEBRIS CONSIDERATION

Job Order 66-520

PREPARED BY

original signed by
Shin-Yi Su, Staff Scientist

original signed by
David M. Oro, Senior Associate Scientist

APPROVED BY

original signed by
A. V. Mazade, Manager
Solar System Exploration Department

Prepared By

Lockheed Engineering and Management Services Company, Inc.

For

Solar System Exploration Division

Space and Life Sciences Directorate

NATIONAL AERONAUTICS AND SPACE ADMINISTRATION
LYNDON B. JOHNSON SPACE CENTER
HOUSTON, TEXAS

August 1985

LEMSCO-21807

ACKNOWLEDGMENT

This report contains many original ideas of D. J. Kessler of NASA's Johnson Space Center. Its completion is the result of his constant attention and encouragement. The authors gratefully acknowledge his cooperation and contributions. Some of the text is extracted from his paper entitled "Earth Orbital Debris."

CONTENTS

TABLES

FIGURES

ABSTRACT

This report begins with a historical review of the evolution of the orbital debris environment resulting from the manmade space objects orbiting around the Earth. A model simulation of the environment is then carried out for the next 35 years both with and without the injection of the Strategic Defense Initiative (SDI) satellites. The effects of the surrounding debris environment on the operation of the SDI satellites are examined. Parametric calculations of the SDI satellite loss rates under various conditions have been performed to evaluate the time scale of the SDI system survivability.

1. INTRODUCTION

As man began to use telescopes to explore the solar system, one of the first phenomena he discovered was that the orbits of all the observable planets are nearly circular and lie in the ecliptic. Moreover, he noticed that the orbits of the moons and the thin rings are circular, too, and lie in the planet's equatorial plane. As the science of orbital mechanics developed, the reasons for these phenomena became clear: these are the only orbits which have any long-term stability. Other orbits are not sustained because the inevitable collisions between objects in these orbits result in the objects' being eventually ground into dust. It has become clear with observations that this process is currently taking place amongst the asteroids as their intersecting orbits cause them to collide and fragment into smaller and more numerous pieces.

Most objects in low Earth orbit are in these unstable orbits, including the orbits of the proposed Strategic Defense Initiative (SDI) satellites ~~proposed for implementation in the year 1995~~. For a close guard against missile leakage, the SDI system requires a large number of satellites placed in closely spaced polar orbits. If left unattended, these satellites will collide with each other and eventually grind themselves into small and numerous fragments. Moreover, even if they are in perfect control to avoid collisions with each other, the surrounding environment is so hazardous that a collision between an SDI satellite and space debris is inevitable. Because of very high collision velocities between the SDI satellites and space debris, a collision will be catastrophic for the SDI satellite. The newly generated collision fragments will start a chain reaction within the closely spaced SDI satellites, and the whole SDI system may be in danger of being destroyed. Consequently, it is important to understand the time scale of this collisional process and the conditions under which the time scale can be changed. It is under such consideration that this report addresses the various aspects of the orbital debris issue. The understanding of the environment and its interaction with the SDI system may be not only a key factor in the design of the SDI satellites but also a decisive factor in the selection of an SDI concept.

2. ORBITAL DEBRIS HISTORY — expand

Orbital debris was first studied in the early 1970's at the Johnson Space Center (JSC) and the Marshall Space Flight Center of the National Aeronautics and Space Administration (NASA). These early studies concentrated only on the less than 2000 objects which were cataloged by the North American Aerospace Defense Command (NORAD) at that time. The major conclusion of these studies was that the collision probabilities, although of some concern, were not significant except for large structures (greater than 100 m in diameter). In the mid-1970's, NASA's Langley Research Center expanded the level of concern by predicting that, as a consequence of explosions in space, the real orbiting population was 2.5 times the cataloged population (ref. 1). In the late 1970's, studies at JSC concluded that fragments resulting from collision between orbiting satellites would be the major source of debris, possibly as early as the 1990's (ref. 2). Later studies (ref. 3) identified explosions of the U.S. Delta rocket second stage and the U.S.S.R. antisatellite weapons as major contributors to the debris in space. As a result, the United States changed the Delta rocket operational procedures to minimize the possibility of future explosions. In 1981 the American Institute of Aeronautics and Astronautics (AIAA) issued a position paper on space debris, concluding that the space debris issue is real and that action must begin now to forestall a serious problem in the future (ref. 4).

Two workshops on the study of space debris have been convened so far. The first was sponsored by NASA-JSC and held in 1982 in Houston. The second was held in conjunction with the 25th Plenary Meeting of Committee on Space Research (COSPAR) in 1984 in Austria. The proceedings of the first workshop were published as NASA Conference Publication 2360 (ref. 5), while the COSPAR workshop proceedings were published as Advances in Space Research 1984 (ref. 6). A third workshop, again sponsored by COSPAR, will convene in 1986 in France.

3. SOURCES OF ORBITAL DEBRIS

3.1 CATALOGED POPULATION

Figure 3-1 shows how the cataloged population has increased over the past 15 years, leading to the official "box score" of 5403 objects in orbit as of December 31, 1984 (ref. 7). It should be noted that not all the 5403 objects are operational payloads. They can be cataloged into four different categories as shown in table 3-1. Nearly one-half of the cataloged objects come from satellite breakups. All but a few of these breakups were explosions - most were accidental, but some were intentional. With only 5 percent of the catalog consisting of the operational payloads, it is obvious that debris control has little to do with limiting the number of operational payloads in orbit.

3.2 UNCATALOGED POPULATION

The first suggestion of a significant uncataloged population was found by comparing the fragment distribution from ground explosions with that detected by NORAD radar (refs. 1 and 3). Based on these types of considerations, it was estimated that between 10,000 and 15,000 objects larger than 4 cm in diameter are in Earth orbit. A report by Johnson (ref. 8) confirms the existence of a significant uncataloged population, based on special tests conducted on the capabilities of NORAD radar detectors.

High-intensity explosions and explosions designed to break up the payload into some particular sizes have the potential of producing a much larger number of smaller objects. It is possible for a single 100-kg payload to break up into 10^5 1-cm objects or into 10^8 1-mm objects. Those small-sized objects are beyond NORAD's ground radar detectability.

Furthermore, unmodeled sources of small debris surely exist. The most likely sources include the material which may be released as a by-product of separation techniques used in orbit. Another possibility is shedding of spacecraft surfaces resulting from material fatigue in space. For example, the thermal expansions and contractions of spacecraft surfaces may cause

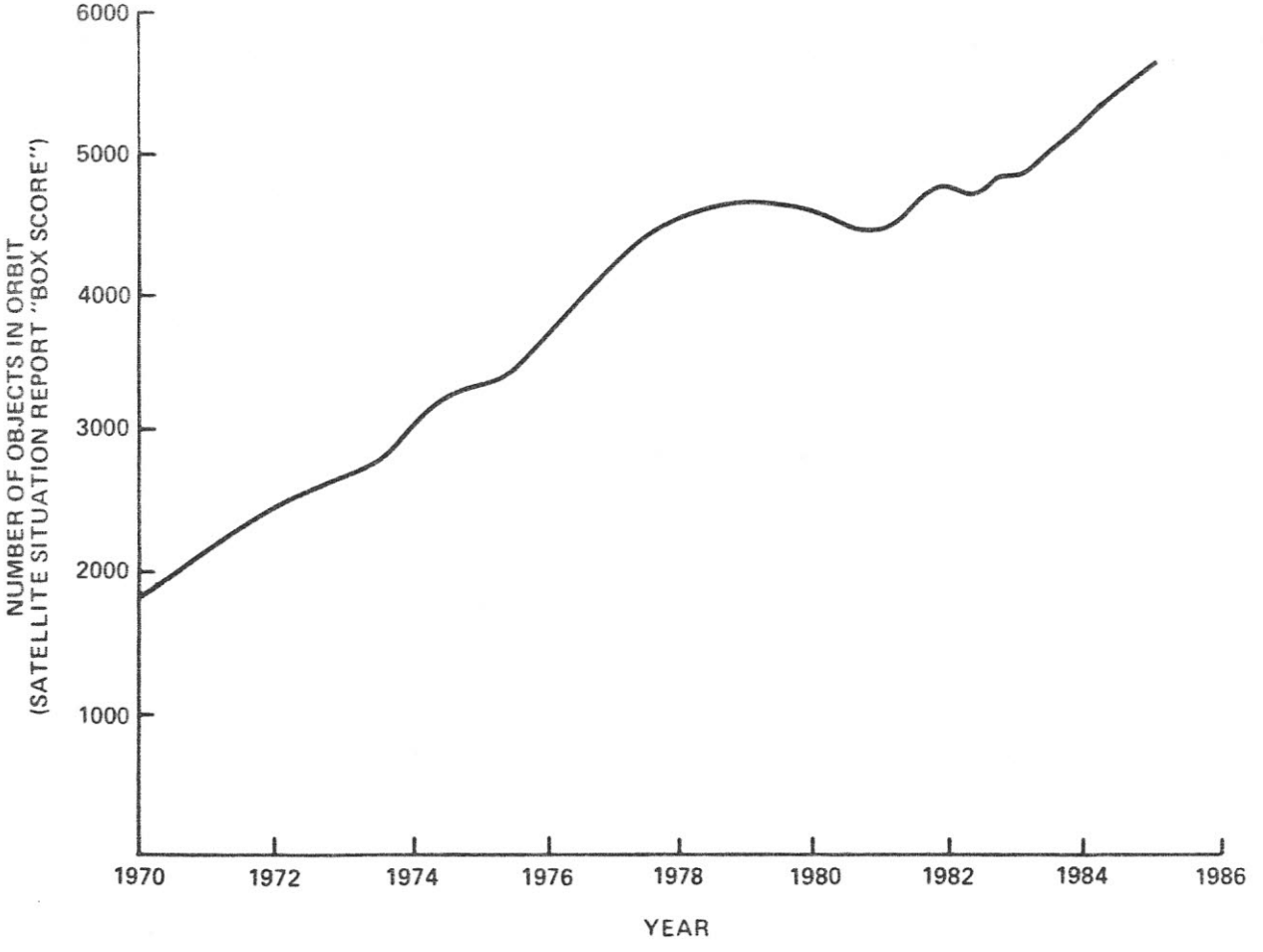

Figure 3-1.- Historical record of objects in space.

TABLE 3-1.- SOURCE OF IN-ORBIT POPULATION CATALOGED BY NORAD

[December 31, 1984, population of 5403 objects]

Space object	Percentage of tracked population in orbit	Notes
Operational payloads	5	Distributions are roughly equally divided between the U.S.S.R. and the U.S.
Nonoperational payloads	21	
Mission related (rocket bodies, shrouds, etc.)	25	
Satellite breakups • Explosions • Unexplained	49	7 Delta stages 4 U.S. other 8 U.S.S.R. satellite tests 4 U.S.S.R. other These 23 breakups account for 93% of the tracked fragments resulting from the 74 known explosions to date.

painted surfaces to flake off slowly. Currently, insufficient data exist to model these potential sources adequately; however, new data from recovered spacecraft, to be discussed in section 4, are becoming available.

4. ORBITAL DEBRIS MEASUREMENTS

Measurements of orbital debris at sizes smaller than those cataloged by NORAD were nonexistent until a few years ago. The first measurements of orbital debris were taken in 1973-74 during the Skylab program. The Skylab Cosmic Dust Experiment S149 and the windows on the returned Skylab IV Apollo Command Module were analyzed. It was discovered that one-half of the hypervelocity craters and pits were aluminum lined (refs. 9, 10, and 11). The size distribution and the frequency of these pits were about what one would expect as a result of debris from solid rocket motors fired in space.

With the beginning of the Orbiter launches, windows were again examined for hypervelocity impacts. However, because these windows are reused, they cannot be used for destructive testing unless they contain a pit too large for safe reuse. Although several windows have been replaced because of pitting, only one has been analyzed, and it contains the largest pit found so far. This pit, first observed by the crew of the seventh Space Transportation System (STS-7) on the third day of flight, contained titanium oxide with traces of carbon aluminum, potassium, and zinc. It was concluded that the particle had a diameter of about 0.2 mm and an impact velocity of between 3 and 6 km/s.

The Explorer 46 Meteroid Bumper Experiment was flown in 1972 to test the effectiveness of the bumper against meteoroids. The very strong directional flux (the number of impacts on an orbiting object per year per square-meter cross-sectional area of the object) measured by this experiment can only be explained by the impacts from the Earth-orbiting population (ref. 12). The experiment was designed to detect particles larger than about 0.1 mm. The orbital debris flux determined by the 43 highly directional impacts is 1.9 impacts/m^2-yr. This is about a factor of 3 below the flux derived from Orbiter window examination, assuming one impact every 50 days in space. The Orbiter window flux is about the same as the meteoroid flux.

Most recently, the returned surfaces of the Solar Maximum Mission (SMM) satellite have been examined. The returned surfaces consist of about 1.5 m^2 of thermal insulation material and 1.0 m^2 of aluminum thermal control louvers.

Analyses of these surfaces are still continuing, but three different types of hypervelocity impacts have been found: meteoritic material, paint particles (consisting both of titanium and zinc pigments with potassium silicate binders and of an unknown chlorine source), and particles of unknown origin (aluminum droplets were detected, but these could have originated from the aluminized surfaces) (ref. 13). Future analysis of these surfaces is expected to provide a more definitive result of the debris environment for sizes smaller than about 0.2 mm.

Early studies within NASA determined that ground-based telescopes could be used to detect orbiting debris 1 cm in size. NASA has contracted Lincoln Laboratories to use their two 31-in. telescopes to search for this kind of small debris. The two telescopes, located 60 m apart, were pointed near the zenith just after sunset and just before sunrise. The results of this search revealed a population 8 times the cataloged population, or about 40,000 objects which are 1 cm or larger (ref. 14). These measurements are summarized in figure 4-1 and compared with the meteoroid environment. Note that in all cases the measured debris environment is comparable to, or exceeds, the meteoroid environment.

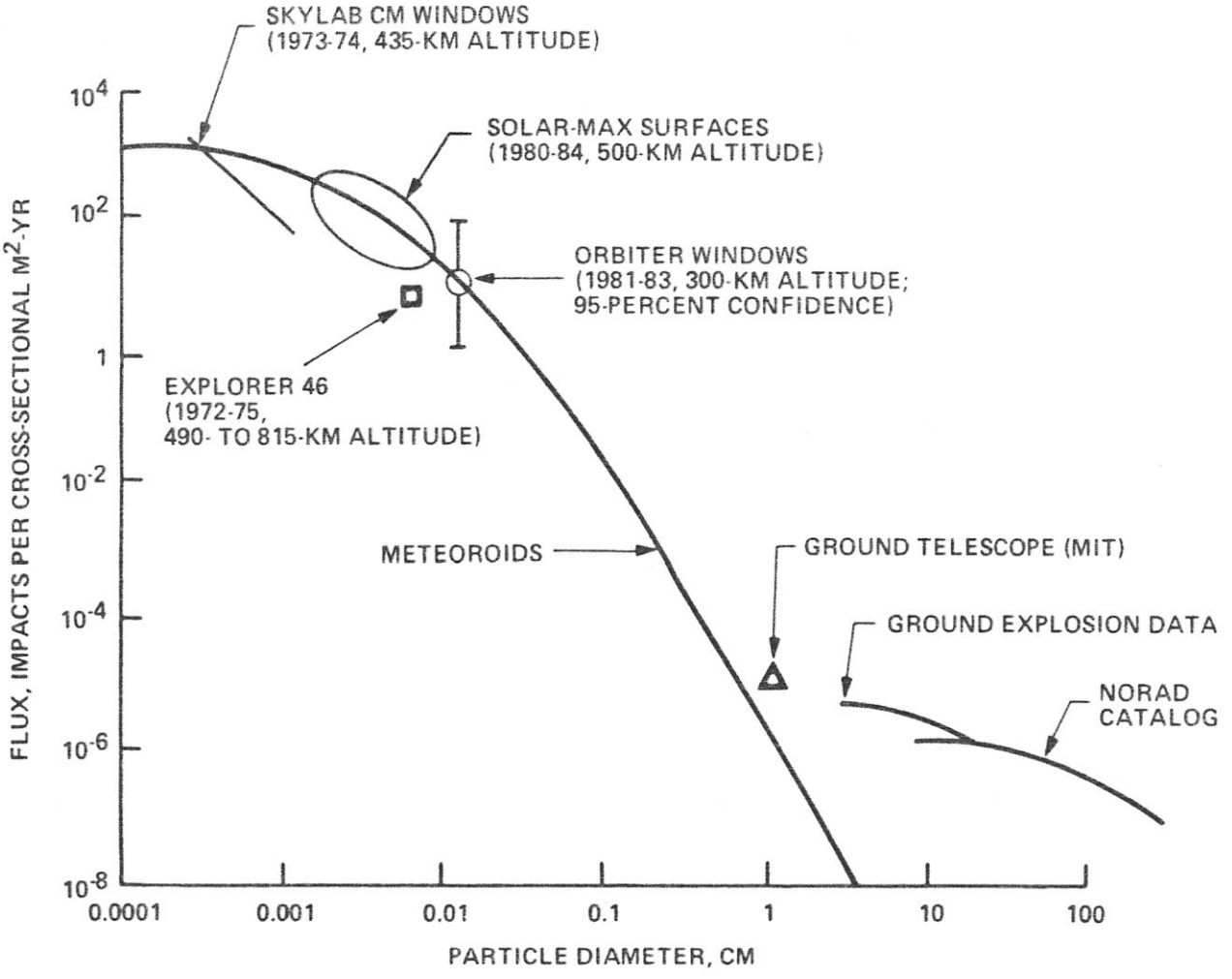

Figure 4-1.- Existing orbital debris measurements compared to meteoroid flux.

5. CONCEPT OF SDI OPERATIONS

Table 5-1 lists two different logistics models of SDI operations. These two models represent the two extreme cases of SDI operations. Because Model A operates at an altitude below 1000 km where most space objects exist, it will be examined in greater detail. Consider the SDI satellites in the 500-km altitude band, for example. There are 37 planes, each of which has an inclination of 87.9° and contains 74 equally spaced satellites. Figure 5-1 shows portions of the planes that are in the Northern Hemisphere projected onto the equatorial plane.

It is assumed, based on the information available, that the planes are equally spaced such that at the Equator they have a separation of 4.86° (584 km) and are oriented such that the satellites are traveling northbound in the Eastern Hemisphere and southbound in the Western Hemisphere. Each satellite has a separation of 4.86° (594 km) with its neighbors on the same orbital plane, and travels at an orbital velocity of 7.61 km/s. The distance between satellites of different planes varies greatly, especially when passing over the poles. At time t = 0, a satellite in the first plane is located on the equatorial plane, whereas a satellite in the adjacent plane is located at half the intersatellite distance (292 km) above the equatorial plane. This scheme is repeated for the remaining planes.

It should be noted that since the satellites of a plane are equally spaced around that plane the orientation of the satellites will return to the initial condition in the time it takes for the satellites to travel the intersatellite distance, which is approximately 77 sec.

The central portion of figure 5-1 is enlarged in figure 5-2 to show the closeness of the SDI satellites around the pole. Between the latitudes of 86.9° and 87.9°, the average density of satellites is one satellite every 6783 km^2.

TABLE 5-1.- SDI LOGISTICS MODELS

Model	Components	Number of satellites	Number of orbital planes/satellites	Cross-sectional area, m^2	Altitude, km	Inclination, deg
A	Kinetic energy weapons (KEW's)	2738	37/74	3.55	500	87.9
		2738	37/74	2.01	600	87.9
		2738	37/74	2.47	700	87.7
		2738	37/74	2.69	800	87.6
	Surveillance (SURV)/C^3	96	4/24	96.02	1100	90.0
D	Direct energy weapons (DEW's)	100	10/10	824.67	1700	70.0
	Escorts (KEW's)	2738	37/74	4.34	1600	90.0
		2738	37/74	4.34	1650	90.0
	SURV/C^3	66	3/22	95.02	1700	90.0

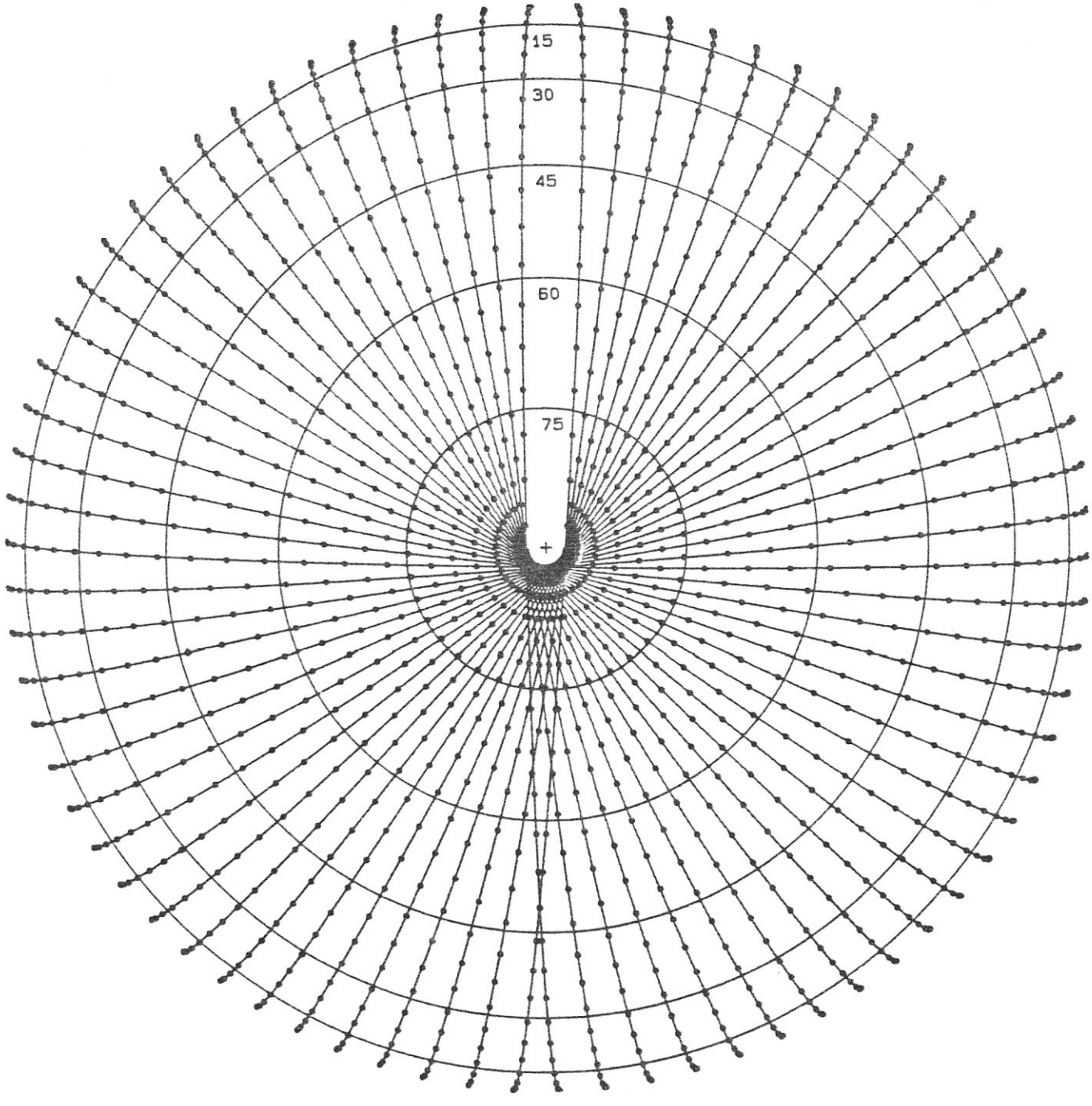

Figure 5-1.- Representation of SDI satellites in the Northern Hemisphere projected on the equatorial plane. Each dot represents one SDI satellite in an orbital plane.

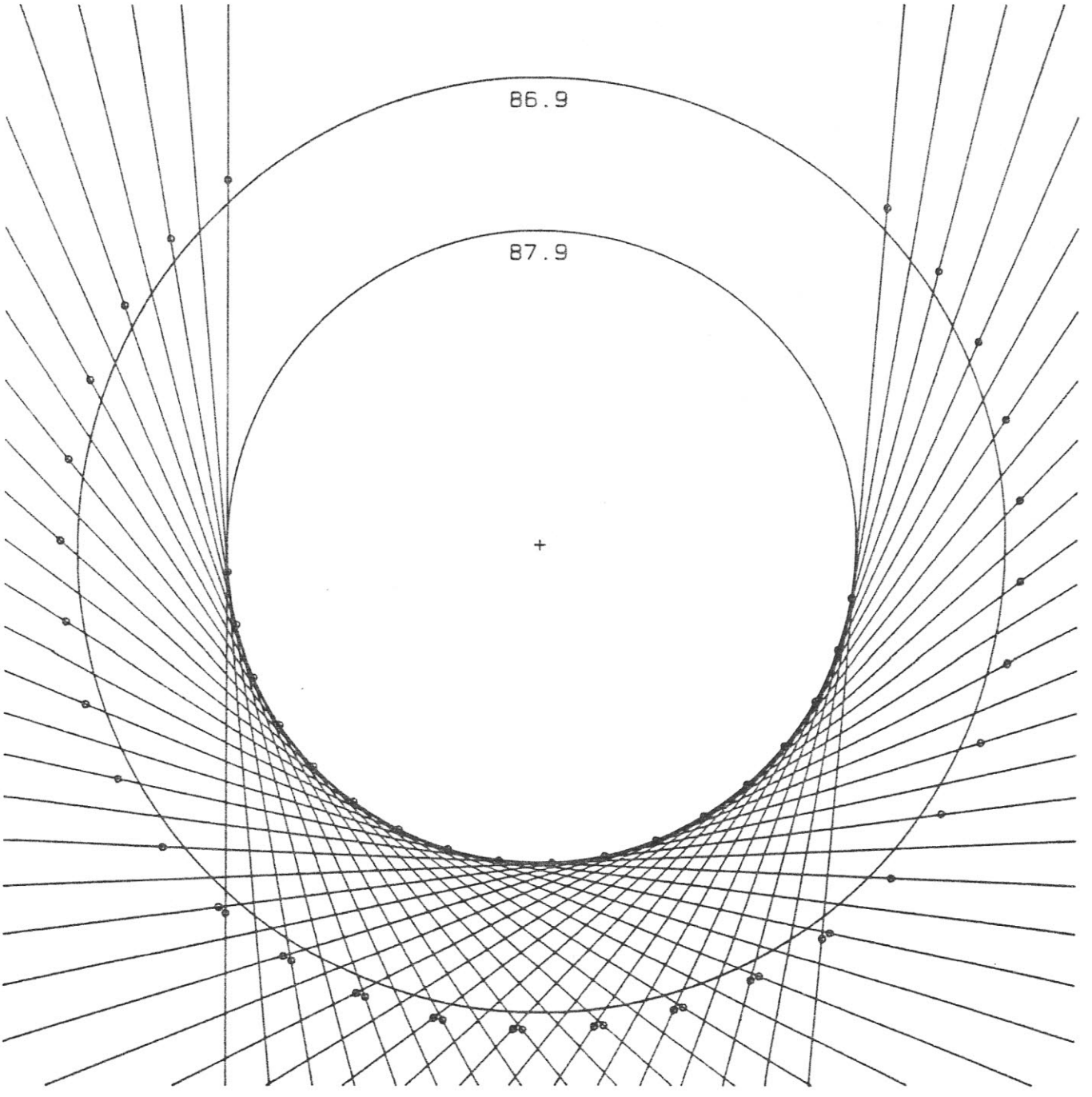

Figure 5-2.- Enlargement of the equatorial projection of SDI satellite tracks near the polar region shown in figure 5-1. When a satellite in one particular orbital plane is located at the 87.9° latitude circle, two satellites are offset and located at the lower latitudes (≈86.9°) at the adjacent orbital plane either side of that particular orbital plane.

The average distance between adjacent satellites in this region is 82 km. This is the best case and is independent of both time and the orientation of the orbits. Actually, the density of satellites increases as one nears 87.9°. If 37 satellites were equally spaced along the 87.9° latitude, the distance between neighbors would be 42.8 km. Furthermore, collisions are most likely to occur in the polar region where the orbits intersect.

6. HYPERVELOCITY IMPACT BETWEEN SDI SATELLITES AND SPACE DEBRIS

Although the SDI satellites are capable of maneuvering to avoid collision between themselves, they are exposed to the hazard of collisions from other space debris passing through their altitudes. No existing detector system, in space or on the ground, is capable of detecting and predicting objects in the 1-mm to 4-cm size range to be in a collision course with the SDI satellites. Furthermore, the SDI satellites are subject to intrinsic failures in orbit, and the failed satellite may drift out of control and run into other SDI satellites.

From the latest laboratory test on the hypervelocity impact of a simulated cylindrically shaped spacecraft body (39 in. long, 11 in. diameter) by a cylindrical projectile (2.5 in. long, 2.3 in. diameter) at 3.5 km/s, the number-size-velocity distribution was obtained for the collision fragments tabulated in table 6-1 (ref. 8). These results were then scaled according to impact energy and momentum when applied to the collision process between the SDI satellites and a space object. In general, there are more smaller sized fragments than larger ones, and the smaller fragments are ejected with higher velocity than the larger ones. Although the magnitude of the ejecta velocity can be measured, the directional distribution of the ejecta has not been modeled. Currently, all the collisional fragments are assumed to be ejected isotropically with respect to the point of impact.

A collision between an SDI satellite and a 4-mm object could produce tens of thousands of objects greater than 1 cm in diameter. All of these collision fragments will return to the point of impact after one revolution around the Earth if the minor orbital precession is ignored. Immediately, this increases the probability of collisions between the fragments and the remaining SDI satellites. Furthermore, because the fragments are ejected isotropically, there will be many fragments whose ejecta velocities have large velocity components perpendicular to the orbital plane of the SDI satellites. For these fragments, the orbital elements will then be the same as the orbital elements of the SDI satellite except for the longitudes of the ascending nodes. In other words, some of the newly generated debris fragments will be

TABLE 6-1.- COLLISIONAL FRAGEMENTS OF A 39- BY 15-IN. SIMULATED SPACECRAFT OBJECT IMPACTED BY A 2.5- BY 2.3-IN. PROJECTILE AT 3.5 KM/S

Debris size, cm	Number* of fragments exceeding the size in column 1	Velocity* of projectile, km/s
(1)	(2)	(3)
10	20	0.02
4	100	.08
0.4	2000	.4

*The energy and momentum scaling law will be used to produce the number-velocity distribution for the simulated SDI fragmentation process.

confined to the same orbital altitude as the operational SDI satellites. These fragments will have an extremely high probability of colliding with the rest of the operational SDI satellites around the polar region where the orbital planes intersect. Thus, after one collision, with so many fragments either residing in or passing through the SDI altitude band, the collision probability for the remaining SDI satellites jumps many orders of magnitude. A chain reaction could then result, and the entire SDI population could be eliminated in a few years.

7. DEBRIS MODEL WITH AND WITHOUT SDI SATELLITES

The model of the Earth orbital debris environment is used to predict the evolution of the debris from 1983 to 2020. This model is used to study the interaction between the SDI satellites and the existing debris population. The SDI satellites are assumed to be placed into orbit in 1995.

In the model, orbiting objects are organized into a group of bins based on the size of the object, the semimajor axis, and the eccentricity of the orbit. Near-Earth space is divided into concentric-shell elements, each with a thickness of 50 km, extending from the ground to an altitude of 2500 km. The average collision rates between objects in different size bins and between objects within a size bin are calculated for each volume element using equations derived by Kessler (ref. 15). These rates, in conjunction with a model of collisional fragmentation based on ground explosion data reported by Bess (ref. 16) and Johnson (ref. 8), are then used to calculate the number of failures that occur and the amount of debris that is generated from these collisions. This debris is then spread over the adjoining volume elements and allowed to collide with other objects. The calculations are performed using a 1-yr time interval.

The model begins with the population of objects in the NORAD catalog as of March 1983. The amount of debris smaller than the sizes tracked by NORAD is extrapolated from the existing debris using the ground explosion data reported by Bess (ref. 16). It is assumed that there will be no explosions in the future that would significantly enhance the debris population, such as the explosions of Delta rockets and antisatellite weapons that occurred in the past. It is also assumed that a constant launch rate equal to that of 1982 will be maintained in future years, with the exception of the launch of SDI satellites in 1995. The only sink of debris in the model is the decay of orbits because of atmospheric drag. For a detailed description of a similar model, see Su and Kessler (ref. 17).

7.1 CASE 1: BACKGROUND ENVIRONMENT

First, the debris environment for the case where no SDI satellites are placed into orbit is described. This background case illustrates the evolution of the debris population assuming no increase in the launch rate, no future explosions, and no SDI satellites. Figure 7-1 shows the flux as a function of altitude for the year 1996 for four different size ranges of debris objects. The size ranges are for objects with diameters greater than 1 mm, 4 mm, 1 cm, and 4 cm. Figure 7-2 shows the results of the background case for the year 2020. The figures show about an order of magnitude increase in the flux of particles greater than 1 mm in diameter from 1996 to 2020. The increase for the other size ranges is less. One can see from the figures that an Orbiter-sized spacecraft at 1000 km will be hit by an object 4 mm or larger once every 16 years by the year 2020.

Figure 7-3 shows the results of the background case as a function of altitude and time for the objects larger than 4 mm in diameter. In this figure one can see that, even with no increase in the launch rate, no future explosions, and no SDI satellites, the debris population steadily increases over a period of years. The major source of objects smaller than 4 cm in this case is the collisions between old rocket motors, dead payloads, and fragments resulting from explosions prior to 1982. The cumulative number of collisions to date from 1980 to 2030 for different sizes of space objects is shown in figure 7-4.

7.2 CASE 2: IMPLEMENTATION OF SDI MODEL A

The average model is now used to determine the survivability of the SDI Model A satellites and their effects on the debris population. Several assumptions are made in this case:

1. The orbits of all working SDI satellites are actively controlled and maintained so that atmospheric drag does not degrade their orbits. Also, due to the control, there are no mutual collisions between working satellites.

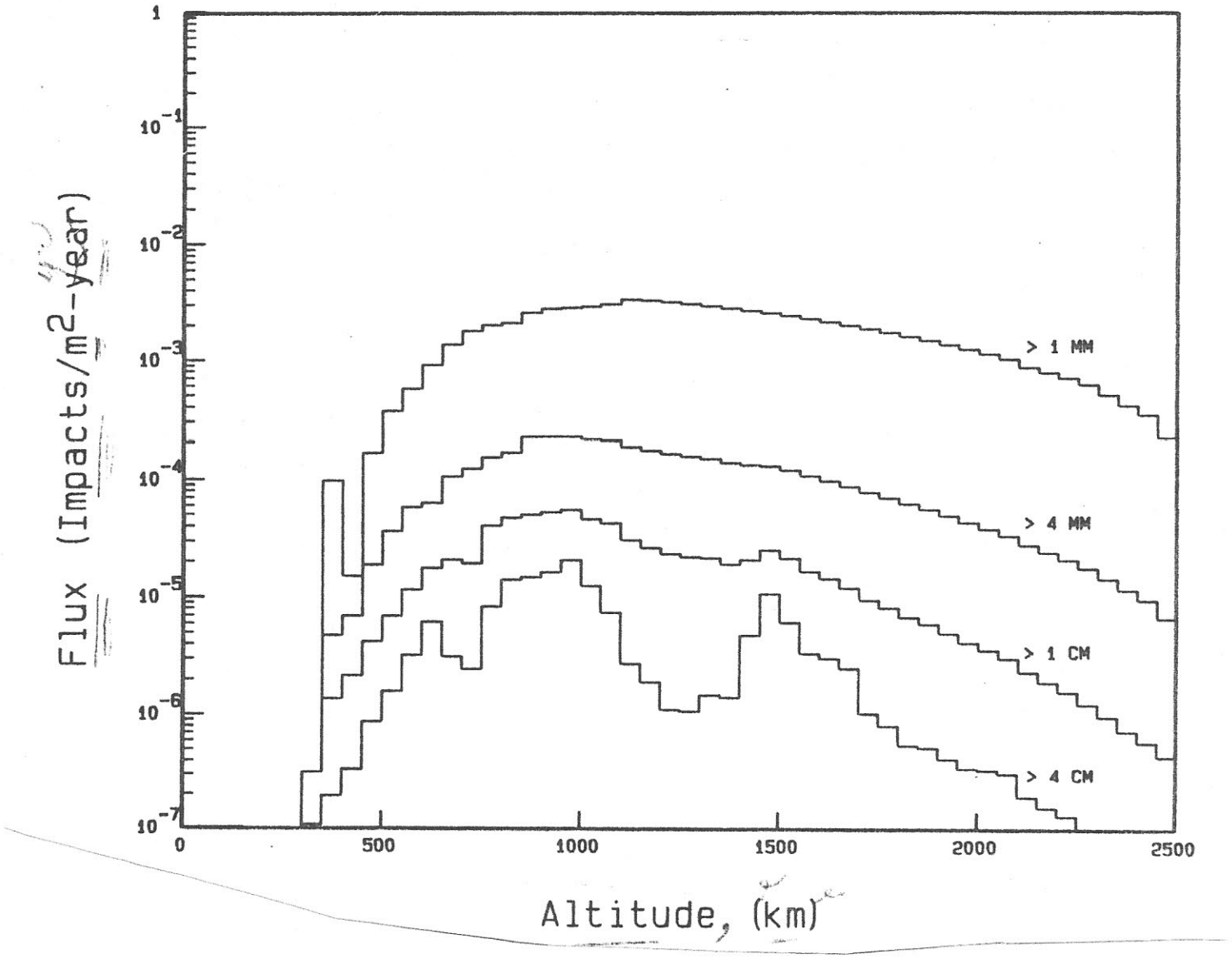

Figure 7-2.- Flux of background debris in 2020 for the case where no SDI system is implemented.

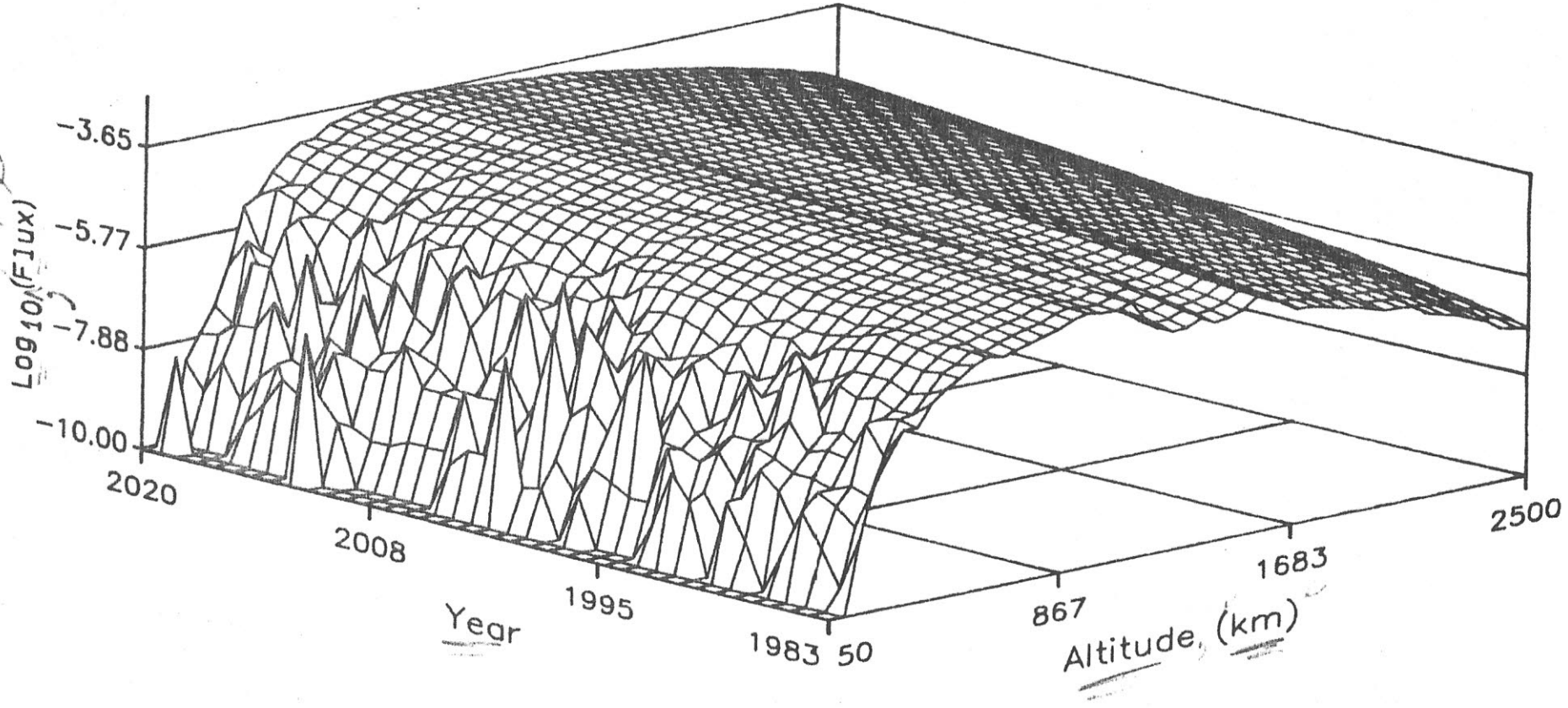

Figure 7-3.- Time evolution of the flux of debris larger than 4 mm in diameter for the case where no SDI system is implemented. The perturbations at low altitudes are due to atmospheric drag competing against the formation of debris.

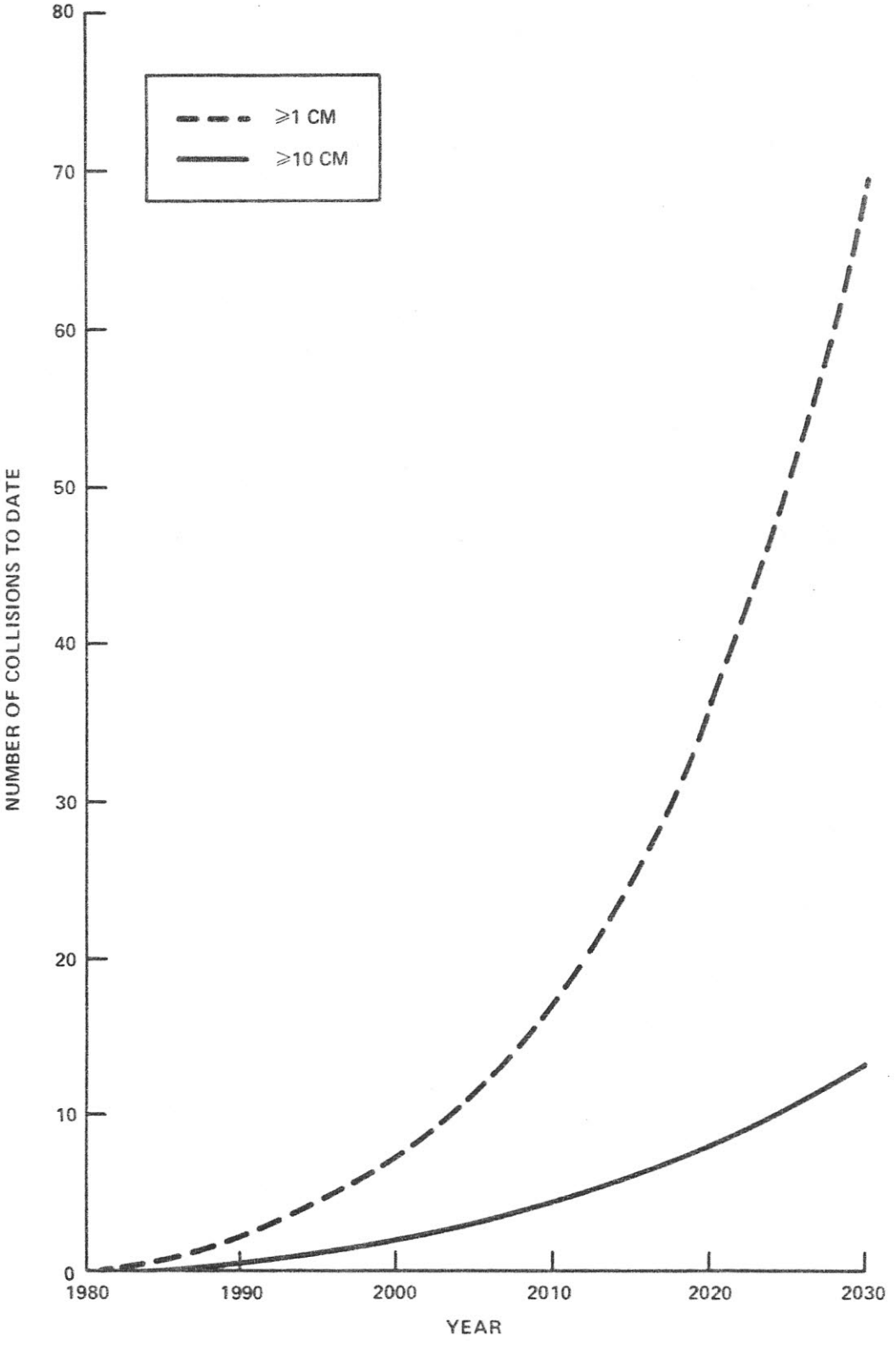

Figure 7-4.- Cumulative number of collisions to date assuming no SDI system is implemented, a constant launch rate equal to that of 1982, and no future spacecraft explosions.

2. One percent of the SDI satellites are considered to be nonworking at any one time. These failed satellites are unable to control their orbits and are allowed to collide with working satellites and other failed ones.

3. The satellites that fail, as well as the 1 percent of nonworking satellites, are not repaired or replaced by new satellites. They are allowed to drift in space, thereby contributing to the debris environment. If they are replaced without being removed from orbit, the debris environment would worsen because of the increased number of objects in orbit.

4. Impacts of debris objects 4 mm in diameter and larger on an SDI satellite cause the failure of that satellite. The satellites can be protected against objects of greater size. However, this protection actually has an adverse effect on the survivability of the satellites, as is explained later in this report.

5. The SDI satellites are placed in orbit such that the bandwidth at each altitude band is only 2 km. A larger bandwidth decreases the rate of collisions, but it increases the difficulty of maintaining the proper positions of the satellites relative to each other.

Figure 7-5 shows the debris flux in 1996, 1 year after the injection of the SDI satellites. One can see a marked increase over the background flux for the same year (figure 7-1). There are distinctive peaks in the flux at the altitude bands of 500, 600, 700, and 800 km for the larger size ranges. This concentration of debris is due mainly to the injection of SDI satellites and due partly to the fragmentation of SDI satellites because of their collisions with existing debris and nonworking satellites.

Figure 7-6 shows the debris flux for the year 2020, 25 years after the injection of the SDI satellites. At this point, all the SDI satellites at the 500-km altitude band, as well as 32 percent at 600 km, 55 percent at 700 km, and 64 percent at 800 km, have failed because of debris collisions. The difference in the percentage of failures is due primarily to the different cross-sectional areas of the satellites in the different altitude bands. A larger cross-sectional area results in a larger collision rate. From the figure, one can see that by 2020 the flux of debris is about 100 times larger than the

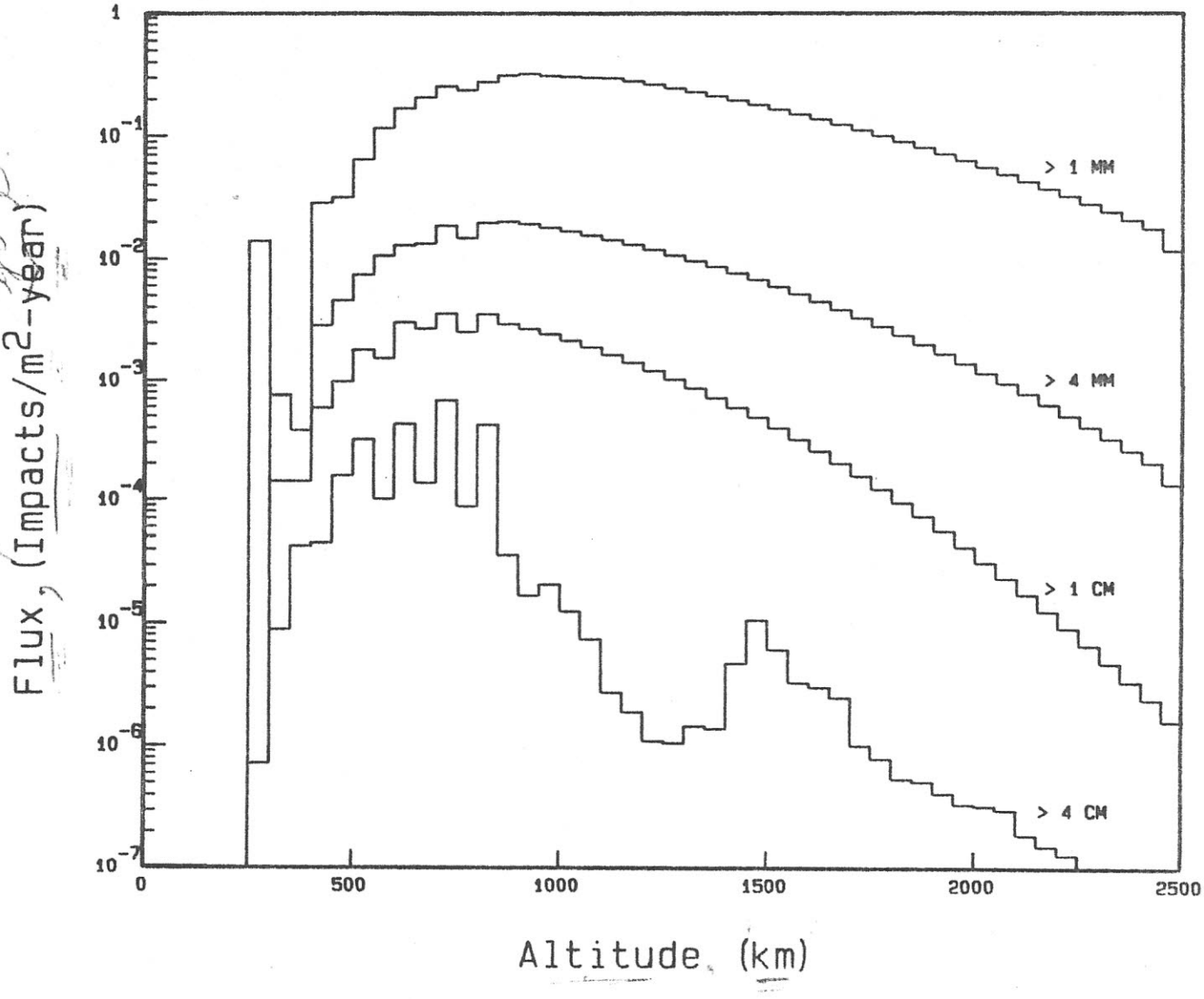

Figure 7-6.- Flux of debris in 2020 for the case where SDI Model A is implemented in 1995. The flux levels are about 2 orders of magnitude larger than the background level for this year.

background flux for this year (figure 7-2). The collision rate for objects greater than 4 mm on an Orbiter-sized object has increased from once every 16 years for the background case to about five collisions per year in this case. No peaks appear for the smaller sizes because of the higher ejection velocity of the smaller debris, resulting in a larger altitude spreading of the debris. Figure 7-7 shows the time evolution of the debris greater than 4 mm in diameter.

7.3 CASE 3: IMPLEMENTATION OF SDI MODEL D

In the third case, the consequences of implementing SDI Model D in 1995 are briefly discussed. The assumptions used for SDI Model D are the same as those previously listed for SDI Model A, with the exception of the altitude bandwidth. In this case the width of each altitude band is 50 km rather than 2 km.

Figure 7-8 displays the debris flux for 1996. The flux level is about the same as that of the background for this year (figure 7-1) with the exception of the peak at 1700-km altitude. This peak is due to the large number of SDI satellites that occupy this region. Figure 7-9 depicts the flux levels for the year 2020. The flux levels are about 100 times larger than the background level (figure 7-2) except for the large peak centered at 1700-km altitude, where the flux level for objects greater than 4 cm in diameter is about 1000 times larger than the background level. No spacecraft operations are feasible in this region, given that an Orbiter-sized object would be hit by a 4-cm or larger object about once a year at this altitude. Figure 7-10 shows the time evolution of the debris greater than 4 mm in diameter. The result indicates a catastrophic impact on the future of the debris environment with the implementation of SDI Model D in the 50-km altitude bandwidth. Confining the satellites to a 2-km bandwidth would only make the situation more severe.

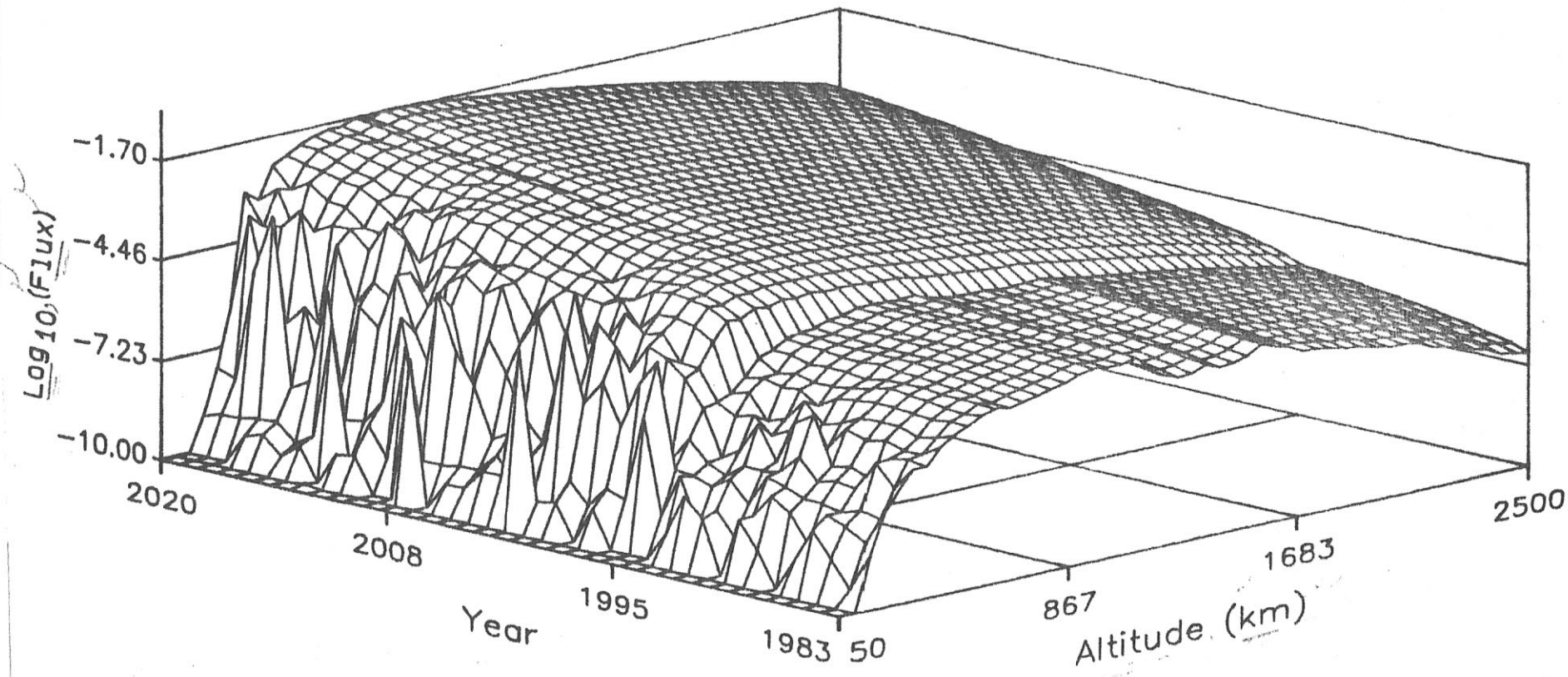

Figure 7-7.- Time evolution of the flux of debris larger than 4 mm in diameter for the case where SDI Model A is implemented in 1995.

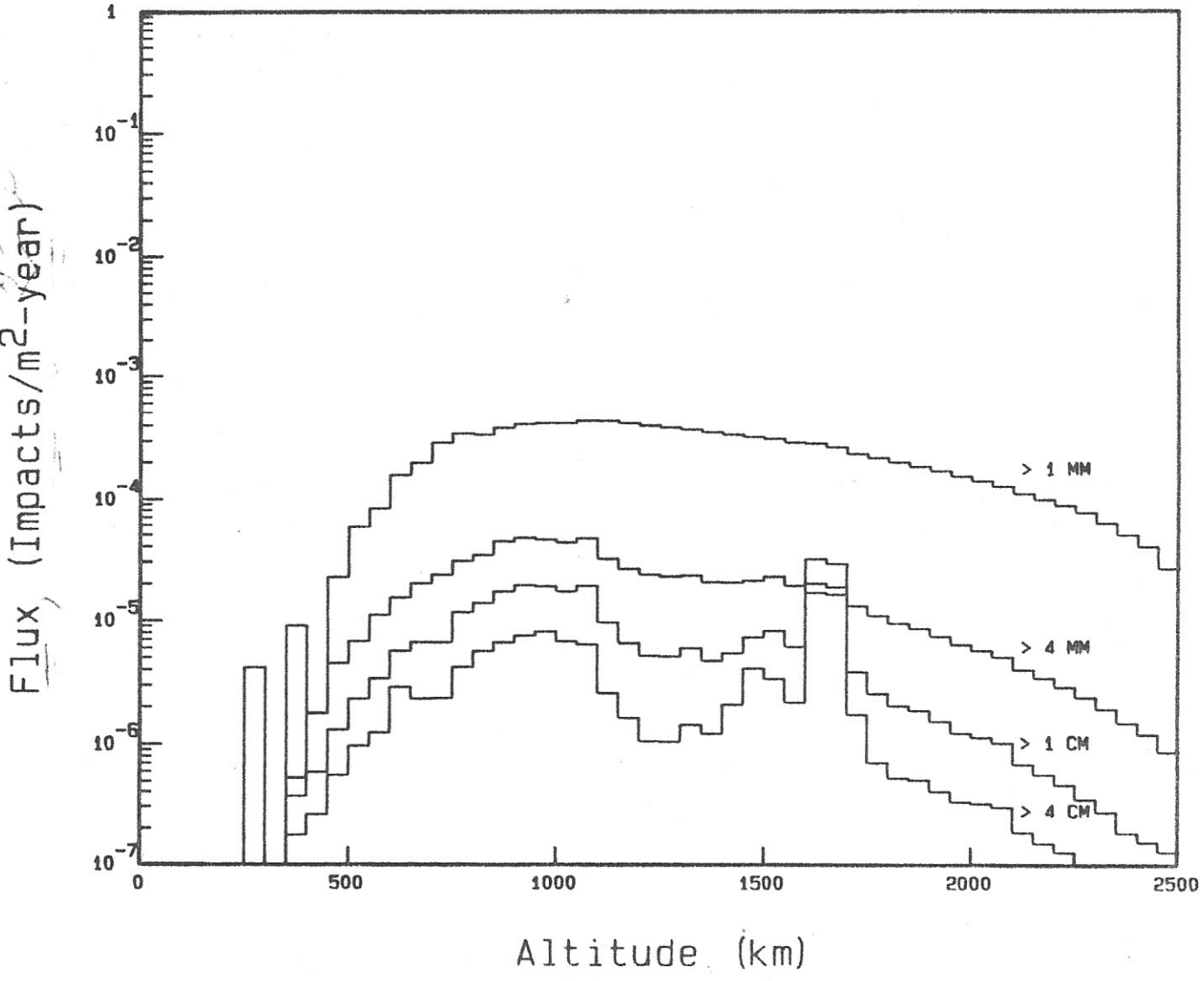

Figure 7-8.- Flux of debris in 1996 for the case where SDI Model D is implemented in 1995. The large peaks for the larger sized debris centered at 1700 km are due to the large number of SDI satellites at that altitude.

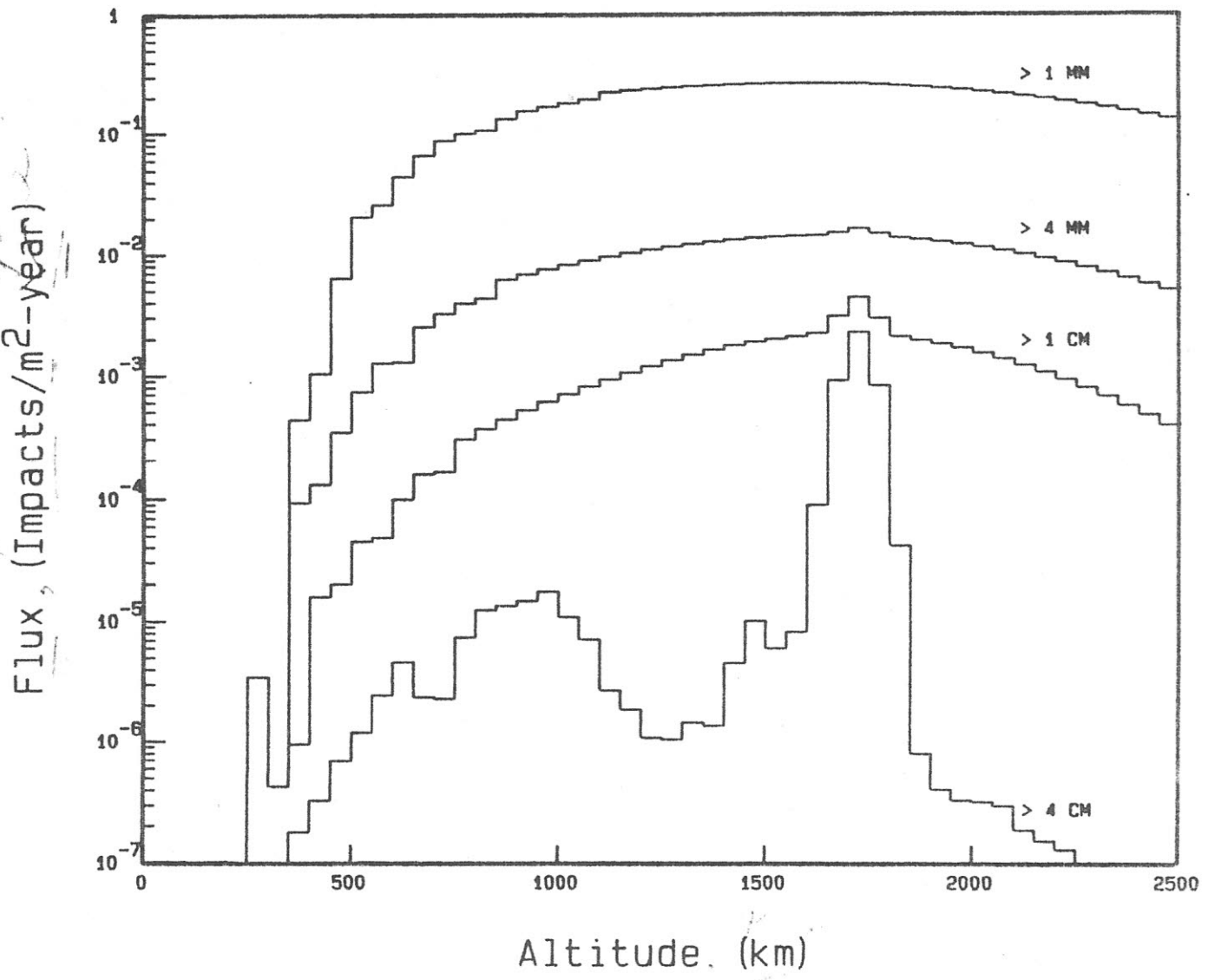

Figure 7-9.- Flux of debris in 2020 for the case where SDI Model D is implemented in 2020. The peak at 1700 km for objects larger than 4 cm in diameter has grown to be 3 orders of magnitude greater than the background level. Successful operation of spacecraft in this region is unlikely.

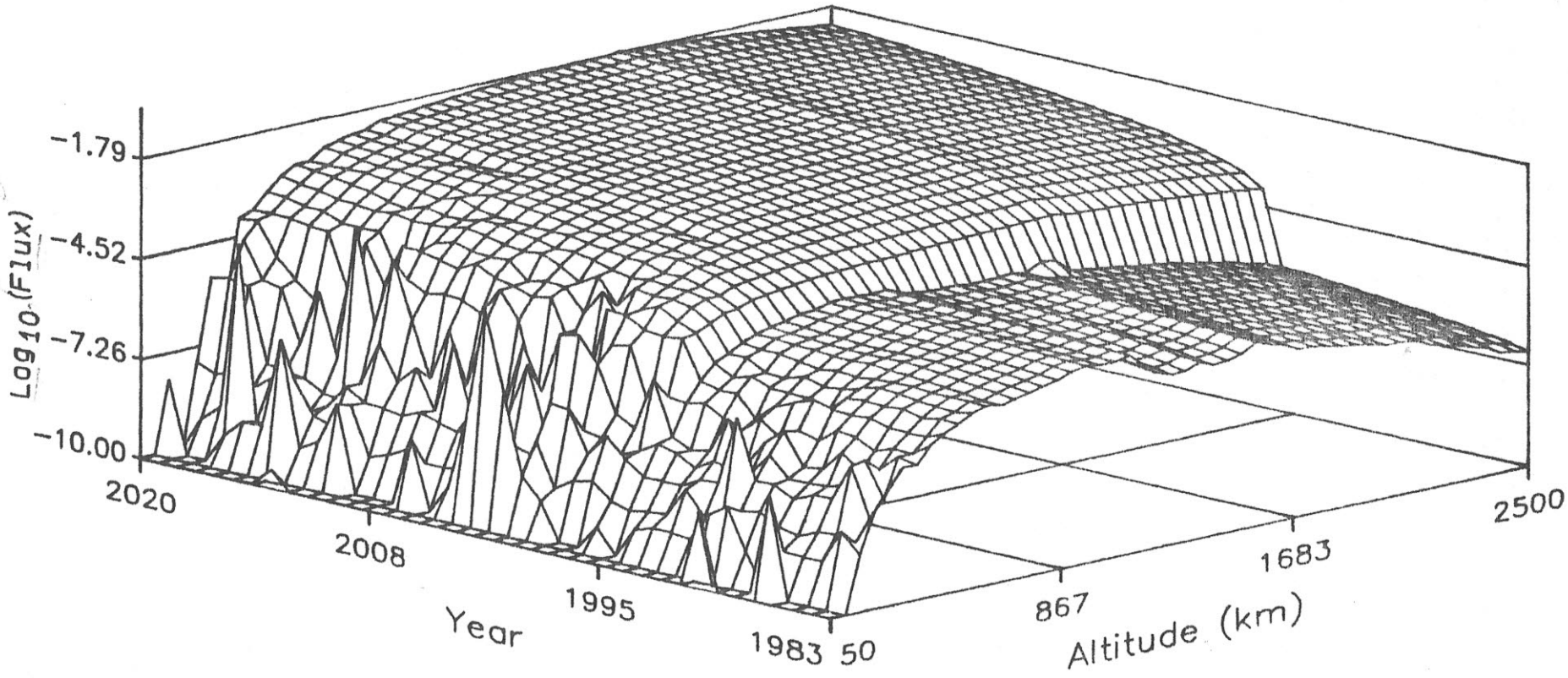

Figure 7-10.- Time evolution of the flux of debris larger than 4 mm in diameter for the case where SDI Model D is implemented in 1995.

8. SIMPLIFIED DEBRIS MODEL FOR CALCULATING SDI SATELLITE LOSS RATE

The model described above is computationally intensive, requiring several hours of computer time to examine each case. A simplified version of the average collision rate model is devised to examine the effects of variations in important parameters on the loss rate of the SDI Model A satellites. To reduce the amount of computation required, only the 800-km altitude band is studied. This model generates the same results as the model described above when using the same assumptions. However, for this analysis, it is assumed that the satellites which fail above the accepted intrinsic failure rate due to debris impacts are replaced by new satellites, rather than not being replaced at all, and that the additional failed satellites become part of the debris environment.

The variable parameters are (1) the acceptable intrinsic failure rate, (2) the altitude bandwidth where the satellites reside, (3) the fragmentation process that occurs upon a collision, (4) the debris population in the altitude band, and (5) the debris protection afforded the satellites. Table 8-1 lists the parameters and the range through which they are varied. In the analysis, one parameter is varied at a time while the others are kept at their nominal value.

The intrinsic failure rate is the rate of SDI failures from nondebris causes. SDI Model A has an acceptable intrinsic failure rate of 1 percent. Figure 8-1 depicts the satellite loss rate above the intrinsic failure rate for 0, 1, 2, and 5 percent intrinsic failure rates for the first 10 years. As can be seen from the figure, initially the loss rates of satellites increase almost linearly with time above the intrinsic failure rate. This increase is the result of satellites colliding with existing debris. The collision fragments then contribute to the debris environment and increase the rate of collision and, thus, the rate of failure. However, after a period of time the loss rate becomes exponential, as shown in figure 8-2, even if no intrinsic failures of satellites are allowed.

TABLE 8-1.- PARAMETERS

Variable	Nominal	Minimum	Maximum
Intrinsic failure rate[a]	1%	0%	5%
Altitude bandwidth[b]	2 km	2 km	4 km
Fragmentation process[c]	250 fragments	125 fragments	500 fragments
Debris population[d]	Background	Background	1,000,000 additional fragments
Satellite protection[e]	4 mm/10 cm	4 mm/10 cm	4 cm/25 cm

[a]Rate of failure due to nondebris impact causes.

[b]Width of altitude band of satellite orbits.

[c]"Effective" number of fragments generated from a collision having orbital parameters similar to those of the SDI satellites.

[d]Amount of debris in the region of satellite orbits.

[e]Size of debris which upon collision with an SDI satellite will cause failure/fragmentation.

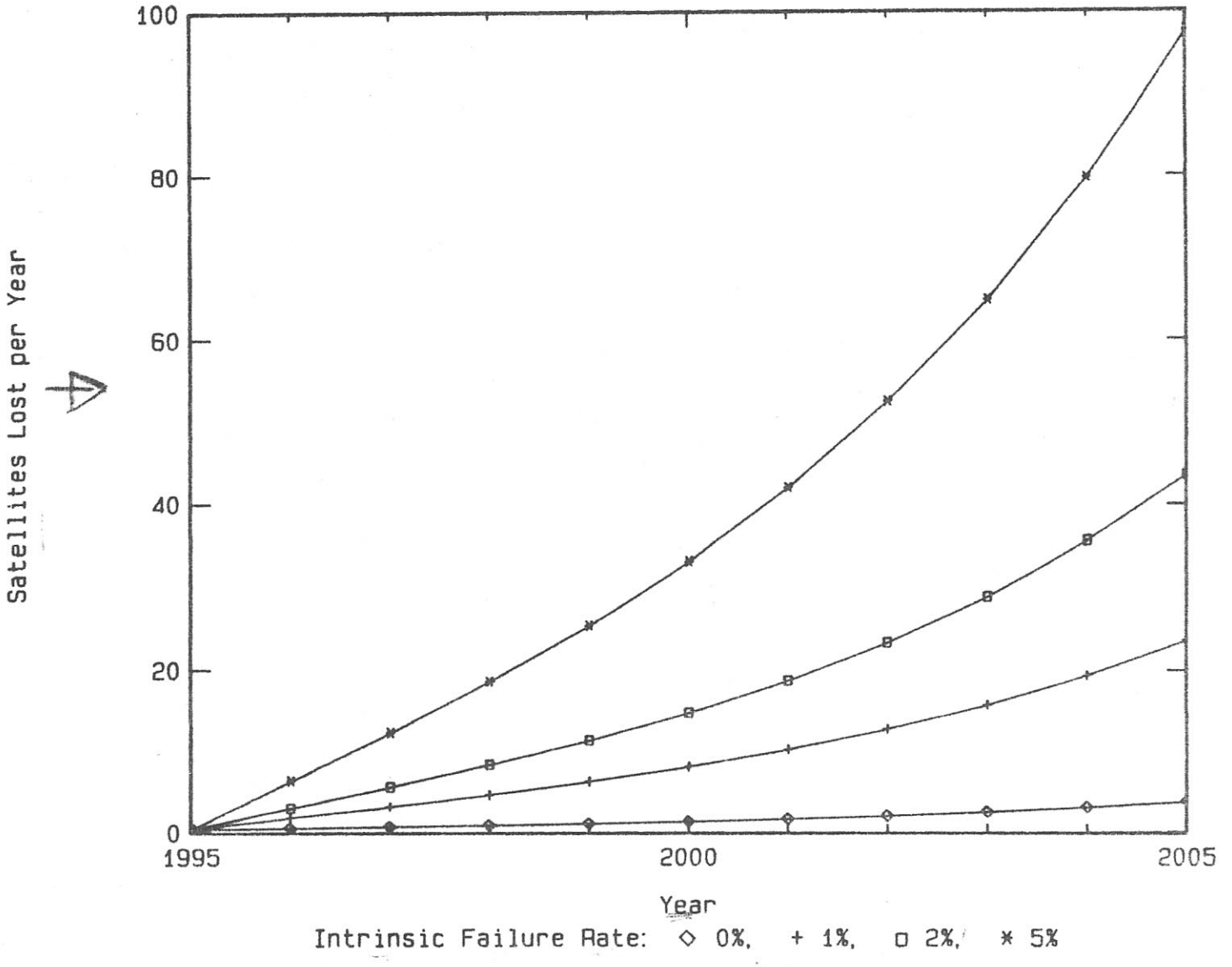

Figure 8-1.- Loss rates for the 800-km altitude band of SDI Model A satellites for the first 10 years after their implementation in 1995. The curves show the number of satellites lost per year above the intrinsic failure rate assuming intrinsic failure rates of 0, 1, 2, and 5 percent, all other parameters being nominal. It is also assumed that satellites which fail because of debris impacts are replaced by new satellites and that the failed satellites are then allowed to contribute to the debris environment.

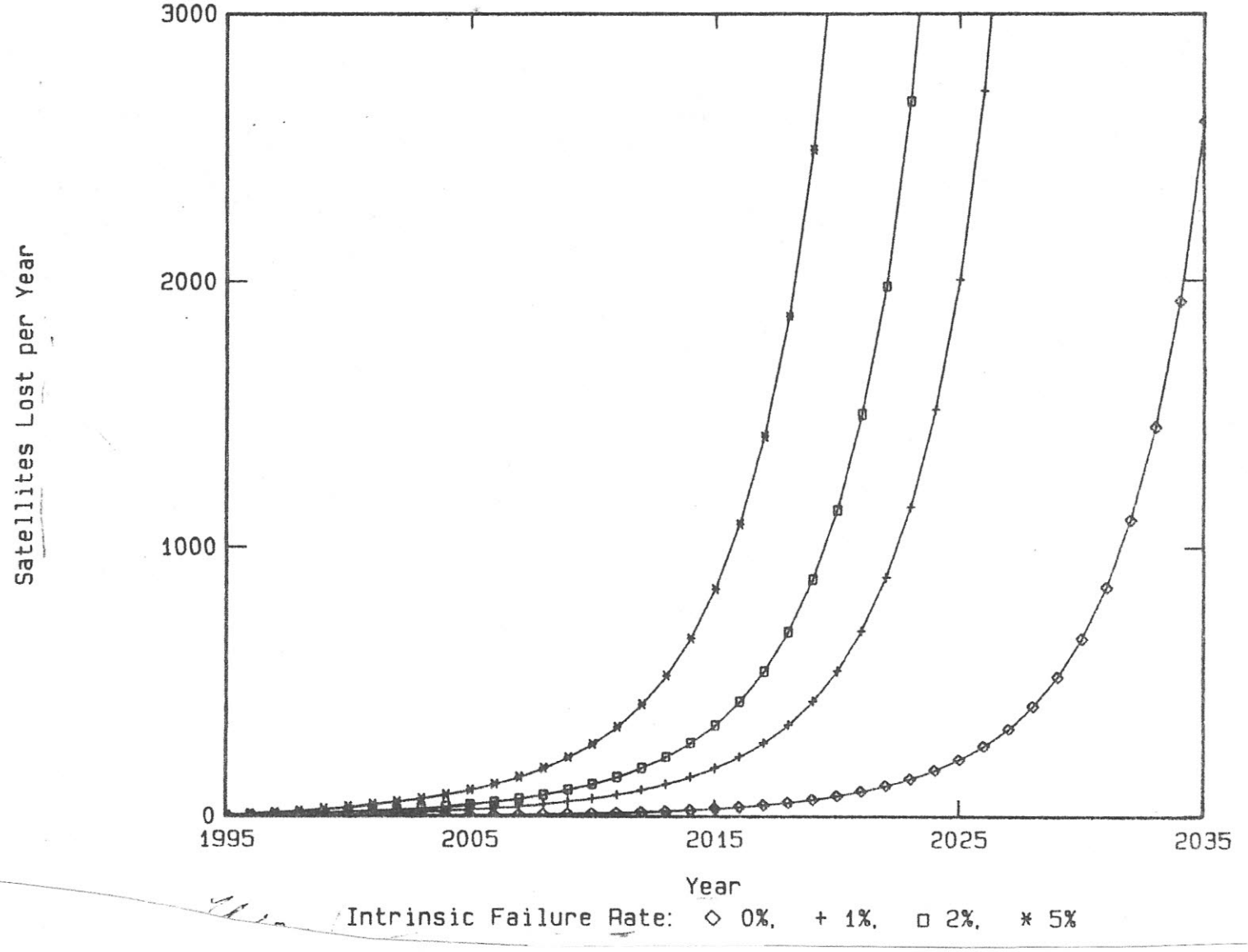

Figure 8-2.- SDI Model A satellite loss rates for the different intrinsic failure rates. The loss rate becomes exponential even if no intrinsic failures of satellites are allowed.

The altitude bandwidth is the range of altitudes over which the SDI satellites are spread. The satellite loss rate is dependent on the altitude bandwidth. This is evident from figure 8-3, in which the failure rates are plotted for the 2-, 3-, and 4-km bandwidths. Optimally, the satellites would be placed in the narrowest bandwidth possible in order to maintain similar orbital parameters. However, a smaller bandwidth causes a higher failure rate. Conversely, a larger bandwidth decreases the failure rate. However, with the larger bandwidths, it will be more difficult to control the positions of the satellites relative to one another.

As discussed earlier in this report, the number-size-velocity distribution of collision fragments has been modeled. However, more important than the total number of fragments generated during a collision is the number of fragments generated whose orbital elements are the same as the elements of the SDI satellites, except for the longitudes of the ascending nodes. These fragments have a very high probability of colliding with other SDI satellites, and their number is dependent on the direction in which the fragments are ejected from the collision point. Currently, there are no measurements of the directionality of collision ejecta, and it can only be assumed that the fragments are ejected isotropically from the impact point. With this assumption and the number-size-velocity distribution of collision fragments, it was calculated that, nominally, approximately 250 fragments large enough to cause future failures will remain in the 2-km bandwidth of the SDI satellites after a collision between an SDI satellite and a large fragment. This "effective" number of fragments depends not only on the way the satellite fragments but also on the bandwidth of the satellite orbits. More fragments are deposited in a larger bandwidth. Figure 8-4 displays the loss rates for nominal, half-nominal (125 fragments per collision), and double-nominal (500 fragments per collision) fragmentation rates for the 2-km bandwidth.

The loss rate is also dependent on the number of debris objects that are in the altitude band of the SDI satellites but that are not the result of SDI satellite fragmentation. The nominal value for this expected background debris population is based on a conservative growth of the existing debris environment. This growth assumes no future explosions of spacecraft and a

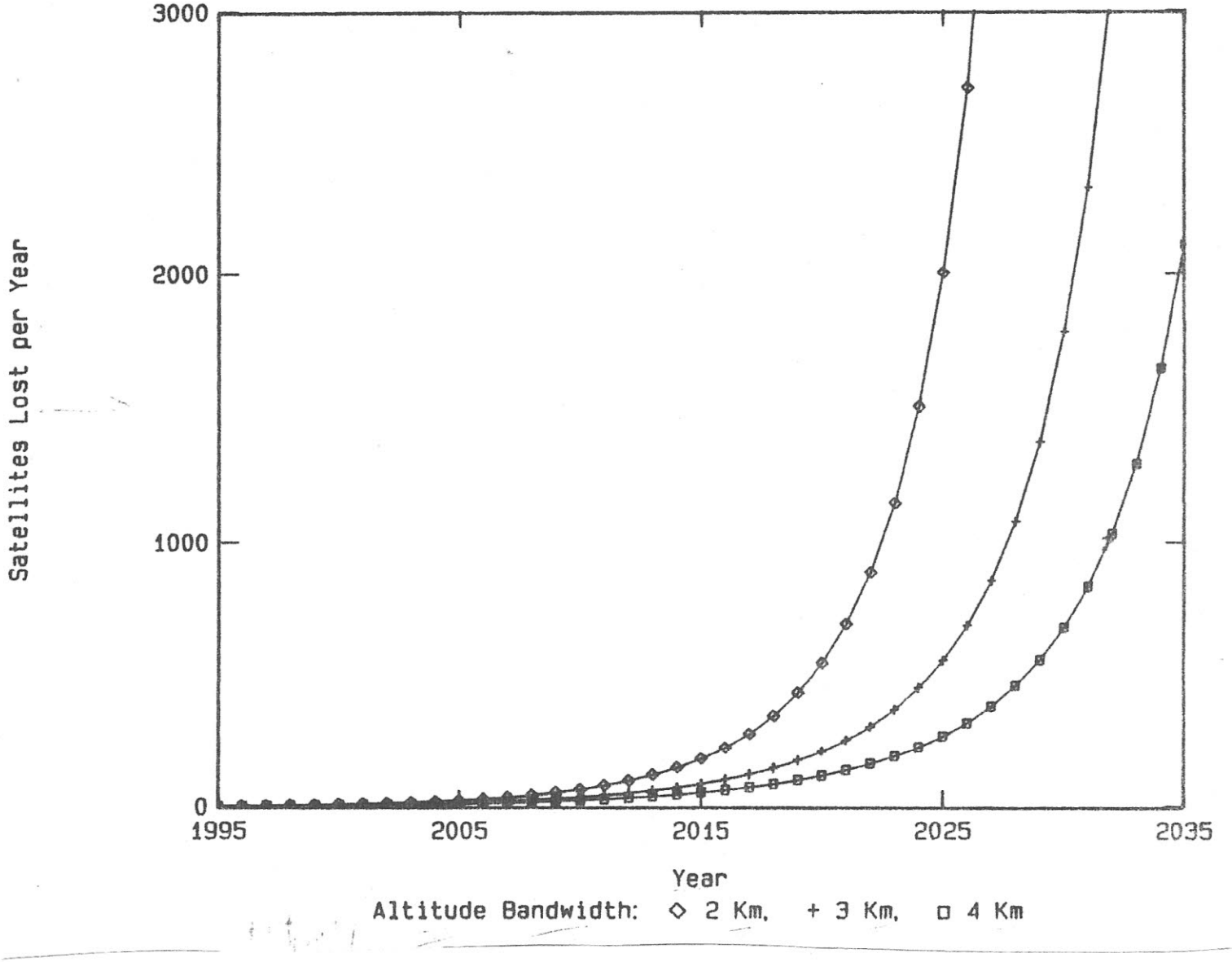

Figure 8-3.- SDI Model A satellite loss rates for altitude bandwidths of 2, 3, and 4 km. The loss rate decreases with increasing bandwidth. However, with larger bandwidths, it will be more difficult to control the positions of the satellites relative to one another.

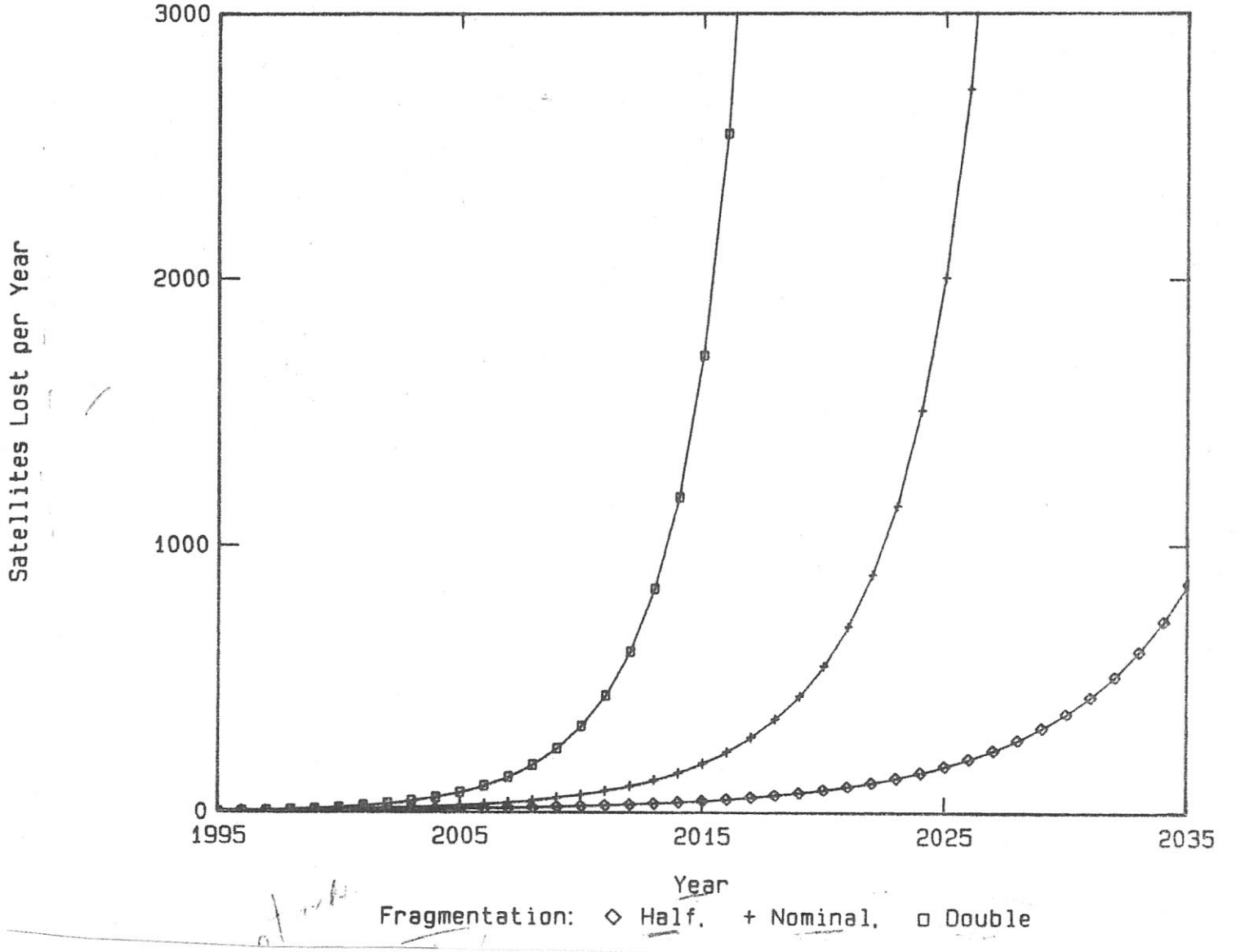

Figure 8-4.- SDI Model A satellite loss rates for half-nominal, nominal, and double-nominal fragmentation of the satellites upon a hypervelocity impact. Nominal has been defined using the results of hypervelocity impact experiments on spacecraft-like structures. Actual fragmentation will depend on a large number of factors, including spacecraft design, collision direction, and impactor material.

constant launch rate equal to that of 1982. A modest increase in the launch rate or the intentional injection of debris fragments into space (perhaps by antisatellite weapons) would significantly increase the debris population and, thus, the loss rate for SDI satellites. Figure 8-5 depicts the satellite loss rates for the nominal debris population and for cases where 10,000, 100,000, and 1,000,000 4-mm debris particles are injected into random orbits in the satellite altitude band. The total mass injections are 1 kg, 10 kg, and 100 kg, respectively. The curves show the destructive effects of injections of relatively small masses of particles.

Above a certain threshold, the failure rate increases with the size of the particle that the satellites are protected against. The strategy for protection is a bumper made of aluminum that is separated from the main body by 25 times the diameter of the debris particle for which protection is desired. The thickness of the aluminum bumper is 0.2 times the diameter of the particle. There is also a layer of aluminum around the main body of a thickness 0.8 times the diameter of the particle. Figure 8-6 shows the relative sizes of two satellites, one protected against up to 4-mm debris, with a cross-section of 2.7 m^2, and the other protected against up to 1-cm debris, with a cross-section of 3.9 m^2. The larger cross-sectional area causes a net increase in the collision rate even though the number of larger fragments is less. This increased rate, coupled with the increased mass of the satellites and the colliding fragment, results in a collision producing more and larger fragments, which are then free to collide with other satellites. The end result is that the SDI satellites fail at a faster rate than if less shielding had been used.

The loss rates for satellites protected against up to 1-cm debris, with a cross-section of 3.9 m^2, are shown in figure 8-7. The curves show the loss rates for the nominal debris population and for cases where 10,000, 100,000, and 1,000,000 1-cm objects (15, 150, and 1500 kg total mass, respectively) are intentionally placed in the satellite altitude band. Figure 8-8 displays the loss rates for satellites protected against up to 2-cm debris, with a cross-section of 6.3 m^2. The curves show the rates for the debris background and for injections of 10,000 and 100,000 2-cm fragments (110 and 1100 kg total

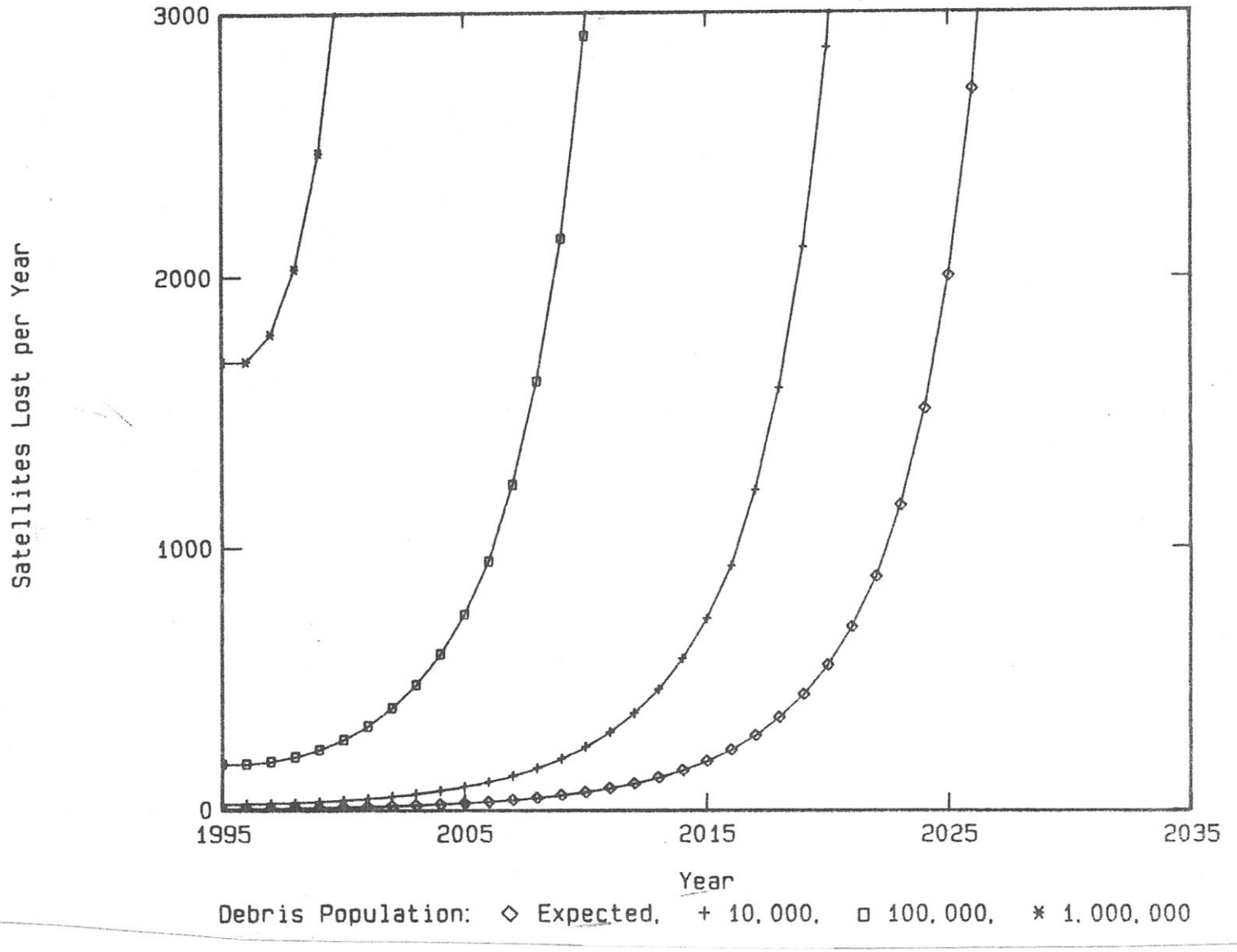

Figure 8-5.- SDI Model A satellite loss rates for various debris levels. These satellites are protected against objects smaller than 4 mm in diameter (nominal case). The curves show the loss rates for the expected background and for cases where 10,000, 100,000, and 1,000,000 4-mm debris objects (1, 10, and 100 kg total mass injection, respectively) are placed into the region of the satellite orbits in 1995. The expected background is derived from the existing debris population assuming a constant launch rate equal to that of 1982 and no future explosions of spacecraft.

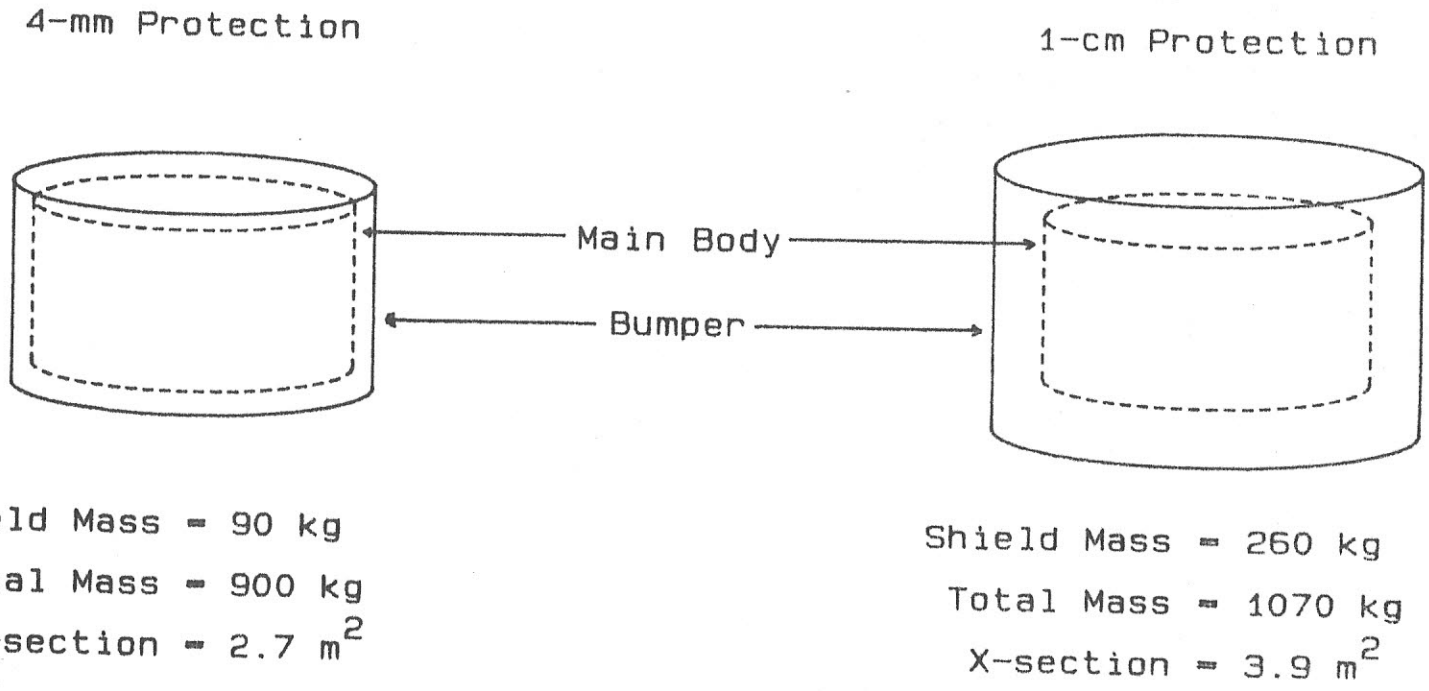

Figure 8-6.- Relative sizes of two satellites. One satellite is protected against objects up to 4 mm in diameter, the other up to 1 cm. The increased protection does not lower the failure rate because of the increased cross-section and mass of the satellite.

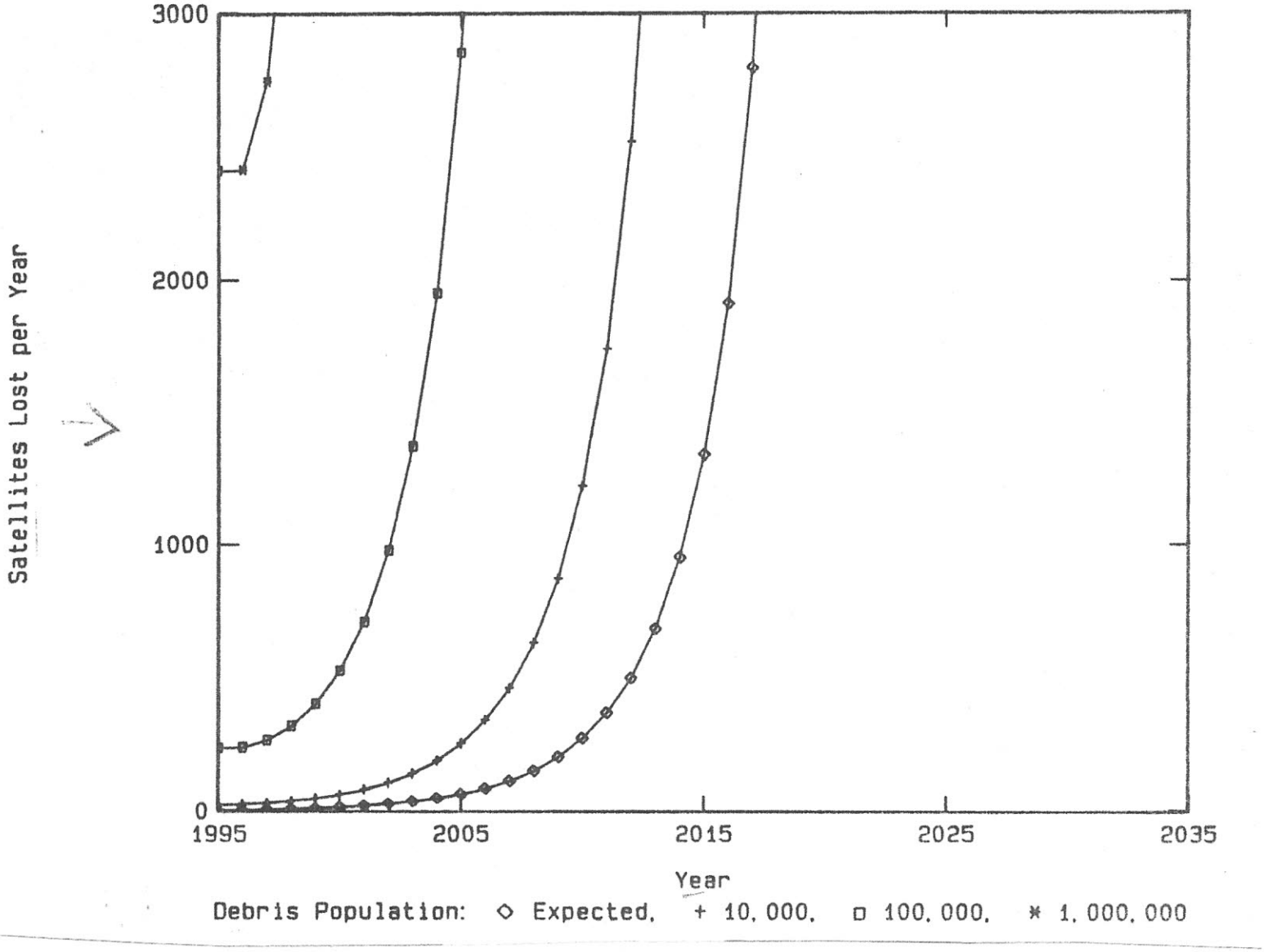

Figure 8-7.- Loss rates for SDI Model A satellites protected against objects up to 1 cm in diameter for various debris levels. The curves show the loss rates for the expected debris background and for cases where 10,000, 100,000, and 1,000,000 1-cm debris objects (15, 150, and 1500 kg total mass, respectively) are placed into orbit at the satellite altitude in 1995.

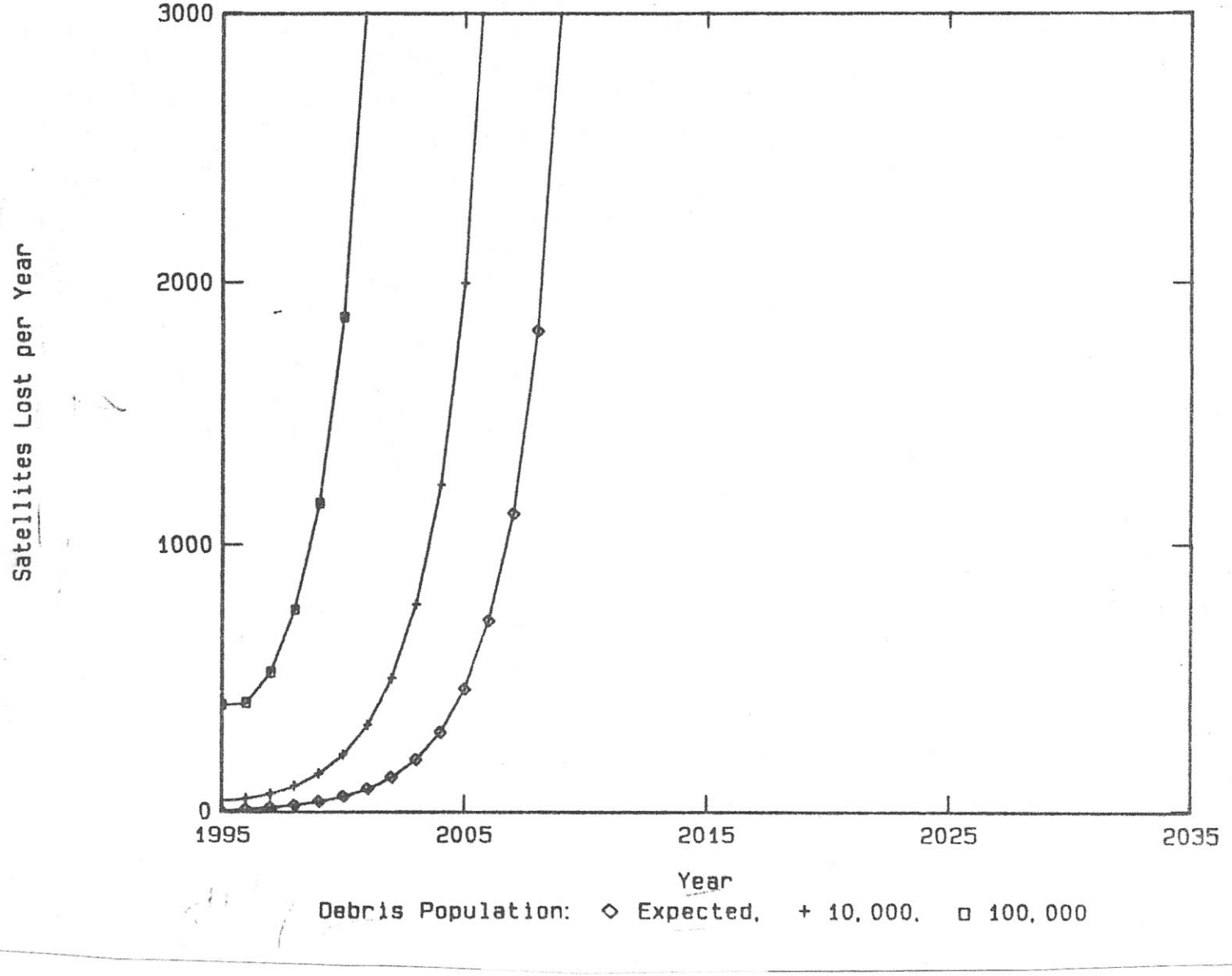

Figure 8-8.- Loss rates for SDI Model A satellites protected against objects up to 2 cm in diameter for various debris levels. The curves show the loss rates for the expected debris background and for cases where 10,000 and 100,000 2-cm debris objects (110 and 1100 kg total mass, respectively) are intentionally placed into orbit at the satellite altitude in 1995. The injection of 1,000,000 1-cm particles (11,000 kg total mass) causes the destruction of 3000 satellites within 9 months after injection.

mass, respectively). The injection of 1,000,000 2-cm fragments (11,000 kg total mass) causes the loss of 3000 satellites within 9 months after injection. Figure 8-9 depicts the loss rates for satellites protected against up to 4-cm debris, with a cross-section of 13 m^2. The curves show the rates for the debris background and for cases where 10,000 and 100,000 4-cm fragments (900 and 9000 kg total mass, respectively) are placed into orbit. The injection of 1,000,000 4-cm fragments (90,000 kg total mass) causes the destruction of 3000 satellites within 4 months. It is evident from these figures that enlarging the cross-sectional area to increase protection can have adverse effects by increasing the collision rate with fragments large enough to cause failure and by actually increasing the failure rate. Obviously, there is an optimum debris size to protect these satellites against that will produce a maximum lifetime. Although no attempt was made to find that size during these analyses, it likely exists in the 1-mm to 4-cm region.

It should be remembered that the results are for one altitude band only. The SDI Model A has four altitude bands to which these results apply.

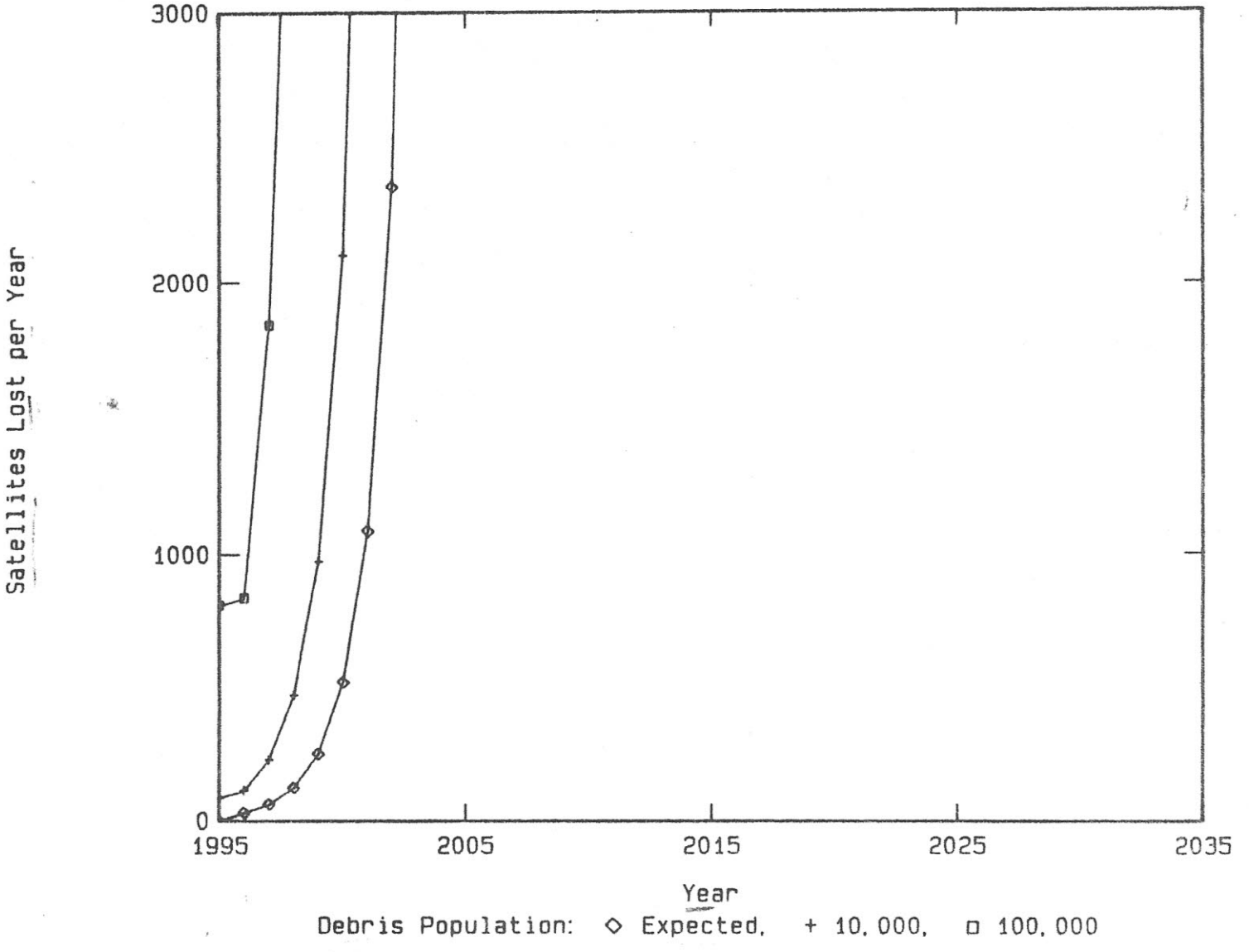

Figure 8-9.- Loss rates for SDI Model A satellites protected against objects up to 4 cm in diameter for various debris levels. The curves show the loss rates for the expected debris background and for cases where 10,000 and 100,000 4-cm debris objects (1000 and 10,000 kg total mass, respectively) are placed into orbit at the satellite altitude in 1995. The injection of 1,000,000 4-cm objects (90,000 kg total mass) causes the destruction of 3000 satellites within 5 months after injection.

9. CONCLUSIONS

From this study, it is obvious that it is important to include the debris issue in the consideration of an Earth-orbiting system of such a large magnitude as the proposed satellite-based SDI system. In this analysis the interaction between the SDI satellites and the debris population was examined, revealing that the evolution of the systems studied leads to catastrophic results on a fairly short time scale. The analysis has also shown that the simple method of deliberately injecting debris into the orbit can significantly increase the rate at which SDI satellites are destroyed.

One of the most important factors in the survivability of the satellites against debris is their cross-sectional area. For this analysis it has been assumed that the satellites are cylindrically shaped, with no external structures such as thermal radiators, solar panels, or launch tubes that would increase their cross-sectional area. It is apparent that the design of a system should strive for the smallest overall cross-section of a system in order to reduce the collision rate and increase the survivability.

Of all the inputs to this study, perhaps the most uncertain is the phenomenon of fragmentation of a spacecraft due to a hypervelocity impact. Whereas the number-size-velocity distribution of ejecta has been modeled from the few laboratory tests on spacecraft fragmentation, the directionality of the ejecta has not been modeled. The directionality is an important factor in determining whether the fragments will remain in orbits that are dangerous to the operating satellites. Also, the structure of the spacecraft is an important factor in the number of fragments that are generated upon a collision. Certain designs may be more prone to fragmentation than others. More tests are required if the uncertainties in these factors are to be reduced.

Also largely uncertain is the amount of debris smaller than 4 cm that is in Earth orbit. The flux for these debris sizes is an important factor in determining the survivability of the satellites. It is the existing debris, along with the intrinsically failed satellites, that act as seeds for the

eventual cascade of collisions and failures. Therefore, it is important to know the exact level of the debris environment. Measurements of the debris in this size range are required to reduce the uncertainty of the amount of debris in Earth orbit.

Up to the present, the debris environment had not been considered an over-riding issue in the implementation of Earth-orbiting systems. Previously, the major debris hazard came from the meteoroid population. With the increase of manmade debris to the level of the meteoroids and the proposal of large-scale orbiting structures such as the Space Station and the SDI satellites, it is clear that the debris environment is becoming an important factor in the design and implementation of orbiting systems. Careful consideration should be given with respect to this environment in the design, implementation, and possibility of success or failure of the proposed SDI systems.

10. REFERENCES

1. Brooks, D. R.; Gibson, G. G.; and Bess, T. D.: Predicting the Probability That Earth-Orbiting Spacecraft Will Collide With Man-Made Objects in Space. Space Safety and Rescue, American Astronautical Society Publications Office (Tarzana, Calif.), 1975, pp. 79-139.

2. Kessler, D. J.; and Cour-Palais, B. G.: Collision Frequency of Artificial Satellites: The Creation of a Debris Belt. J. of Geophys. Res., vol. 83, no. 6, 1978, pp. 2637-2646.

3. Kessler, D. J.: Sources of Orbital Debris and the Projected Environment for Future Spacecraft. J. of Spacecraft and Rockets, vol. 18, no. 4, 1981, pp. 357-360.

4. AIAA Technical Committee on Space Systems: Space Debris. AIAA Position Paper, American Institute of Aeronautics and Astronautics (N.Y.), 1981.

5. Orbital Debris. NASA Conference Publication 2360, 1985.

6. Kessler, D. J.; Grün, E.; and Sehnal, L., eds.: Space Debris, Asteroids and Satellite Orbits. Advances in Space Research, vol. 5, no. 2, Pergamon Press Ltd. (Oxford, UK), 1985.

7. NASA Office of Public Affairs: Satellite Situation Report. Vol. 24, no. 5. Goddard Space Flight Center (Greenbelt, Md.), 1984.

8. Johnson, N. L.: History and Consequences of On-Orbit Breakups. Space Debris, Asteroids and Satellite Orbits, D. J. Kessler, E. Grün, and L. Sehnal, eds., Advances in Space Research, vol. 5, no. 2, Pergamon Press Ltd. (Oxford, UK), 1985, pp. 11-19.

9. Hallgren, D. S.; and Hemenway, C. L.: Analysis of Impact Craters From the S-149 Skylab Experiment. Lecture Notes in Physics, Springer-Verlag (Berlin, Heidelberg, N.Y.), 1976, pp. 270-274.

10. Nagel, K.; Fechtig, H.; Schneider, E.; and Neukum, G.: Micrometeorite Impact Craters on Skylab Experiment S149. Lecture Notes in Physics, Springer-Verlag (Berlin, Heidelberg, N.Y.), 1976, pp. 275-278.

11. Clanton, U. S.; Zook, H. A.; and Schultz, R. A.: Hypervelocity Impacts on Skylab IV/Apollo Windows. Proc. 11th Lunar Planet. Sci. Conf., 1980, pp. 2261-2273.

12. Kessler, D. J.: Explorer 46 Meteoroid Bumper Experiment: Earth Orbital Debris Interpretation. Presented at the IAU Colloquium on Properties and Interactions of Properties and Interactions of Interplanetary Dust (Marseille, France), July 9-12, 1984.

13. Kessler, D. J.; Zook, H. A.; Potter, A. E.; McKay, D. S.; Clanton, U. S.; Warren, J. L.; Watts, L. A.; Schultz, R. A.; Schramm, L. S.; Wentworth, S. J.; and Robinson, G. A.: Examination of Returned Solar-Max Surfaces for Impacting Orbital Debris and Meteoroids. Proc. 16th Lunar Planet. Sci. Conf., 1985, pp. 434-435.

14. Taff, L. G.; Betty, P. E.; Yakutis, A. J.; and Randall, P. M. S.: Low Altitude, One Centimeter, Space Debris Search at Lincoln Laboratory's (M.I.T.) Experimental Test System. Space Debris, Asteroids and Satellite Orbits, D. J. Kessler, E. Grün, and L. Sehnal, eds., Advances in Space Research, vol. 5, no. 2, Pergamon Press Ltd. (Oxford, UK), 1985, pp. 35-45.

15. Kessler, D. J.: Derivation of the Collision Probability Between Orbiting Objects: The Lifetimes of Jupiter's Outer Moons. Icarus, vol. 48, 1981, pp. 39-48.

16. Bess, T. D.: Mass Distribution of Orbiting Man-Made Space Debris. NASA Technical Note D-8108, 1985.

17. Su, S.-Y.; and Kessler, D. J.: Contribution of Explosion and Future Collision Fragments to the Orbital Debris Environment. Space Debris, Asteroids and Satellite Orbits, D. J. Kessler, E. Grün, and L. Sehnal, eds., Advances in Space Research, vol. 5, no. 2, Pergamon Press Ltd. (Oxford, UK), 1985, pp. 25-34.